Journal of Sea Research 103 (2015) 59–74

Contents lists available at ScienceDirect

Journal of Sea Research

journal homepage: www.elsevier.com/locate/seares

Salinity predicts the distribution of chlorophyll *a* spring peak in the southern North Sea continental waters

Xavier Desmit *, Kevin Ruddick, Geneviève Lacroix

Royal Belgian Institute of Natural Sciences (RBINS), Operational Directorate Natural Environment, Gulledelle 100, B-1200 Brussels, Belgium

ARTICLE INFO

Article history:
Received 28 January 2014
Received in revised form 10 February 2015
Accepted 16 February 2015
Available online 11 March 2015

Keywords:
North Sea
Eutrophication
DIN:DIP Ratio
Nutrient Limitation
Nutrient Requirement
Phaeocystis

ABSTRACT

In the North Sea, the coastal waters of Belgium and The Netherlands regularly exhibit intense spring phytoplankton blooms where species such as *Phaeocystis* recurrently form a potential ecological nuisance. In the Belgian and Dutch continental shelves (BCS and DCS), we observe a direct correlation between the chlorophyll *a* spring maximum (*Chlmax*) and the nutrients (DIN and DIP) available for the bloom. As the nutrients are themselves strongly correlated with salinity, a rationale is developed to predict *Chlmax* from winter salinity. The proposed rationale is first tested in a theoretical case with a 3D-biogeochemical model (3D-MIRO&CO). The method is then applied to independent sets of in situ observations over 20 years in the BCS and the DCS, and to continuous FerryBox data in April 2008. Linear regressions explain the relationships between winter nutrients and winter salinity ($R^2 = 0.88$ to 0.97 with model results, and $R^2 = 0.83$ to 0.96 with in situ data). The relationship between *Chlmax* and the available nutrients across the salinity gradient is also explained by yearly linear regressions ($R^2 = 0.82$ to 0.94 with model results, and $R^2 = 0.46$ to 0.98 with in situ data). Empirical 'DIP requirement' and 'DIN requirement' for the spring biomass bloom formation are derived from the latter relationships. They depend i.a. on the losses from phytoplankton during the spring bloom formation, and therefore show some interannual variability (8–12% for DIP and 13–20% for DIN). The ratio between nutrient requirements allows predicting in winter which nutrient will eventually limit the spring biomass bloom along the salinity gradient. DIP will generally be limiting in the coastal zone, whereas DIN will generally be limiting offshore, the switch occurring typically at salinity 33.5 in the BCS and 33.6 in the DCS. N reduction should be prioritized to limit *Phaeocystis* in the coastal zone, with target winter DIN:DIP ratios below 34.4 molN molP^{-1} in the BCS, or 28.6 molN molP^{-1} in the DCS.

1. Introduction

Along the eutrophic North Sea coast of Belgium and The Netherlands, high biomass phytoplankton blooms occur systematically in spring. The onset of the spring biomass bloom is determined by the light availability (Peperzak, 1993; Peperzak et al., 1998), while the magnitude of the chlorophyll *a* spring maximum, *Chlmax*, is commonly considered to be limited by the nutrient availability (Muylaert et al., 2006; Riegman et al., 1992). In the Belgian and Dutch continental shelves (respectively BCS and DCS), nutrient inputs result from the combination of two end-members: the continental freshwater discharges and the Atlantic water inflow (Brion et al., 2006; De Vries et al., 1998; Ruddick and Lacroix, 2006). The nutrient-enriched river waters are the cause of coastal eutrophication, causing nutrient imbalance and ecological disturbances (Jickells, 1998; Lancelot et al., 1987, 2009; Philippart et al., 2007). The relative importance of terrigenous nutrients in the sea increases with the degree of freshwater eutrophication that is sensitive to agricultural practices and water treatment policies at the level of the watersheds (Thieu et al., 2010). The main freshwater sources to the BCS and the DCS are the continental rivers Scheldt, Rhine/Meuse, Seine and Somme. The combination of Atlantic water penetration, freshwater discharge and wind characteristics results in a variety of salinity and nutrient distributions (Ruddick and Lacroix, 2006), which in turn control the spatial distribution of the phytoplankton bloom. The spatial distribution of *Chlmax* in the BCS and the DCS typically shows high values in the coastal zone and a decreasing gradient towards the offshore (de Vries et al., 1998; Los and Bokhorst, 1997; Rousseau et al., 2006; Schaub and Gieskes, 1991, and see Baretta-Bekker et al., 2009 for phytoplankton abundances). Model results indicate that the *Chlmax* spatial gradient might be correlated with salinity (Fig. 1). This suggests a relationship between salinity, dissolved nutrients and chlorophyll *a*, where salinity scales the nutrient concentrations available for the chlorophyll *a* bloom. In this study, we propose to relate *Chlmax* to winter dissolved nutrient concentrations, and to use winter-spring salinity differences as a proxy for nutrient advection during the bloom formation. The correlation between *Chlmax* and the nutrients effectively used allows estimating the nutrient requirement for the spring bloom formation, a concept close but not

* Corresponding author. Tel.: +32 2 773 21 42.
E-mail address: xdesmit@naturalsciences.be (X. Desmit).

http://dx.doi.org/10.1016/j.seares.2015.02.007

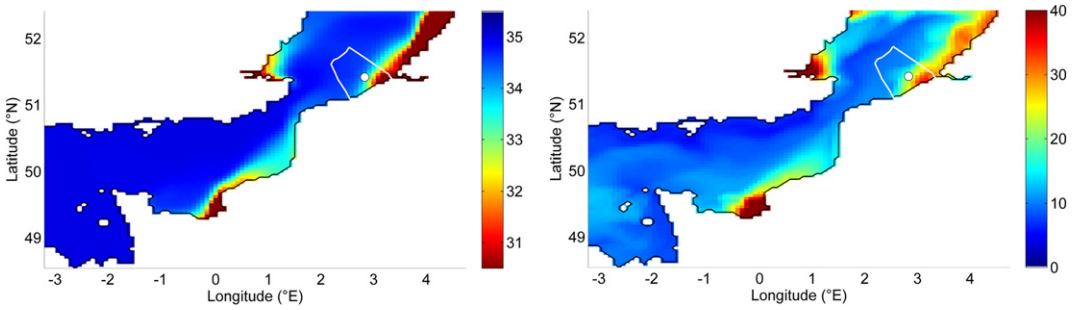

Fig. 1. Results from the 3D-MIRO&CO model. Left — Modeled spring salinity (day 100) in the year 2001 in the English Channel and the southern North Sea. The BCS boundaries are drawn (white line) and the white dot indicates the position of station 330 [51°26.05 N; 02°48.50 E]. Right — Modeled chlorophyll *a* spring maximum (μg L^{-1}) in 2001.

identical to the 'resource use efficiency' proposed in Ptacnik et al. (2008). The simple rationale behind the nutrient requirement offers prediction capabilities for the distribution of *Chlmax* as a function of salinity. It also opens new considerations about the nutrient limitation of the spring phytoplankton bloom in the North Sea. This is a potentially useful tool in the management of eutrophication at policy level when establishing target concentrations for nutrients and chlorophyll *a*.

The near-shore spring bloom (March to May, centered in mid-April) is most of the years dominated by the colonial haptophyte *Phaeocystis globosa* (Rousseau et al., 2012) after the early diatom bloom has been limited by silica (Baretta-Bekker et al., 2009; Breton et al., 2006; Lancelot et al., 1987; Rousseau et al., 2006). Colonial *Phaeocystis* presence in the North Sea was already reported in the late 1890's, and may be seen as a natural phenomenon (Cadée and Hegeman, 2002). However, the duration and cell numbers in these blooms increased at least fivefold over the eutrophication period 1970's–1980's (Jickells, 1998). While *Phaeocystis* is not always considered a harmful species in the same way as toxic algae (Cadée and Hegeman, 2002), it may be the cause of ecological disturbances. Studies on the trophic efficiency in the planktonic food web demonstrated that high *Phaeocystis* abundances ($>4 \times 10^6$ cells L^{-1}) result in the formation of large-size colonies that are inedible to zooplankton copepods (Daro et al., 2006; Rousseau et al., 2000). The recurrent spring-bloom dominance of *Phaeocystis* in the North Sea causes a potential decrease in zooplankton grazing and constitutes a significant loss for higher trophic levels (Lancelot et al., 2009). Therefore it is considered an ecological nuisance and high spring chlorophyll *a* concentrations indicate an undesirable status in the North Sea continental waters.

Efforts in mitigating the effects of eutrophication led to a strong P reduction in the North Sea circa 1990 before concomitant N reductions, and an increase in the DIN:DIP ratios was observed as a result in the BCS and the DCS (De Vries et al., 1998; Soetaert et al., 2006; Vermaat et al., 2008). This nutrient imbalance is in the advantage of *Phaeocystis* dominance over diatoms in the spring (Breton et al., 2006; Gypens et al., 2007). After early-spring diatoms have been limited by silica, *Phaeocystis* may grow on surplus nitrogen, even under low DIP concentrations due to its strong affinity for dissolved organic phosphorus (Schoemann et al., 2005). Model studies concluded that, after the P reductions of the 1990's, further N reductions should be prioritized in order to mitigate *Phaeocystis* nuisance (Gypens et al., 2007; Lacroix et al., 2007a; Lancelot et al., 2007). Adverse effects following the reduction of one nutrient only have already been observed in other coastal ecosystems, and Conley et al. (2009) advise a dual-nutrient-reduction strategy to alleviate eutrophication in aquatic ecosystems. In the present study, indications are given on the DIN:DIP ratio that may potentially decrease *Phaeocystis* dominance in the spring bloom.

Previous authors (Gieskes and Schaub, 1990; Henriksen, 2009; Loebl et al., 2009; Schaub and Gieskes, 1991; van Beusekom et al., 2009) have proposed correlations between annual or seasonal phytoplankton biomass and nutrient concentrations, or river loads, in the North Sea, the Kattegat or the Baltic Sea. De Vries et al. (1998) already plotted long-term averaged summer chlorophyll *a* concentrations versus salinity in the DCS. They observed that cholorophyll *a* increases with decreasing salinity (until 32) and levels off at lower salinities and concomitant higher nutrient concentrations, suggesting that coastal phytoplankton biomass is often light-limited. Muylaert et al. (2006) show a correlation between March nutrients and April *Phaeocystis* chlorophyll *a* in the Belgian coastal zone, suggesting a direct link between the end-of-winter dissolved nutrients and *Chlmax*. However, none of the previous studies attempted to account for the winter-spring advection of dissolved nutrients and their relationship with the problematic spring peak of chlorophyll *a*. This is precisely the topic of the present study. A rationale is proposed to explain through correlations the relationship between *Chlmax* and the winter nutrients that are determined by salinity. This relationship is first tested in a theoretical case with *Chlmax* and nutrients resulting from a biogeochemical model (3D-MIRO&CO; Lacroix et al., 2007b). Then, the method is applied to field observation data obtained from in situ national monitoring programs over the period 1991–2010 in the BCS and in the DCS, and from ODAS-FerryBox continuous recordings in April 2008.

2. Methods

2.1. Rationale

The rationale of the present study is that, in the southern North Sea continental waters, the limiting nutrient (N or P) at the end of the winter is converted from the dissolved phase to phytoplankton biomass (with losses) and hence determines the chlorophyll *a* spring maximum. In a fixed location, between the end of the winter and the spring chlorophyll *a* peak, the changes in dissolved nutrient are mainly related to phytoplankton production or changes in salinity. The latter represents well the advection of enriched freshwater and its mixing with oceanic waters. This can be accounted for by applying a salinity correction to winter nutrients to estimate the 'transported' nutrients, i.e. the potential amount of dissolved nutrients that will be converted into the chlorophyll *a* peak in a given location (Fig. 2a). When the limiting nutrient gets to very low concentrations, the chlorophyll *a* reaches its spring maximum. The non-limiting nutrient remains available at the moment of the peak. To estimate the quantity of limiting and non-limiting nutrients necessary to the chlorophyll *a* bloom peak, a second correction is applied by subtracting the remaining concentrations at the peak from the 'transported' concentrations. This step is particularly necessary for the non-limiting nutrient as it is not completely consumed by the bloom, whereas the correction may be assumed unnecessary for the limiting nutrient if its concentration is close to zero. The result is the 'effective' nutrient concentrations.

The 'effective' nutrient concentration includes a part of nutrient that is lost by processes during the growth period. This implies that the amount of processed winter dissolved nutrients is larger than the amount eventually found in phytoplankton at the chlorophyll *a*

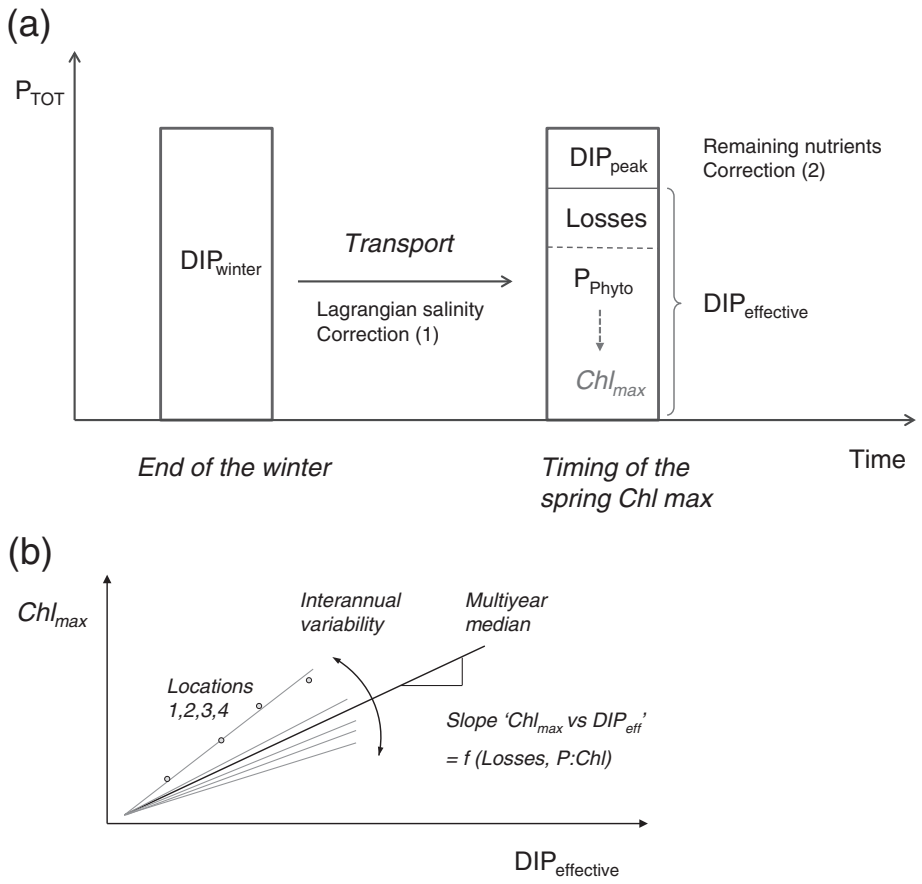

Fig. 2. Scheme illustrating the rationale behind winter-nutrient conversion into spring chlorophyll *a*. (a) The nutrient resource 'effectively' used by phytoplankton to form the spring peak is known by applying two corrections on winter nutrients: a first correction (1) based on salinity to account for nutrient transport during the growth process; and a second correction (2) to account for the remaining nutrients at the peak. The chlorophyll *a* spring maximum mainly relies on this amount of 'effective' nutrients and on the losses endured during the spring growth. (b) A linear correlation may be drawn each year between the chlorophyll *a* maximum and the 'effective' nutrient concentrations. The slope may vary from year to year around a central tendency. A multiyear median slope with its measure of variability may be used for predicting the chlorophyll *a* maximum at any spring salinity.

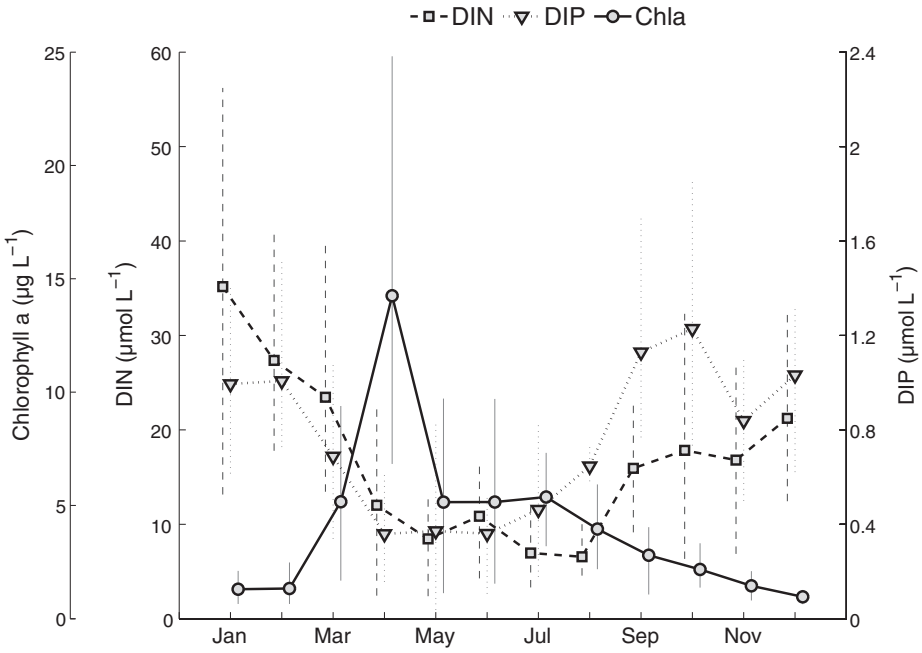

Fig. 3. In situ data from Belgium Marine Data Center (BMDC). Multiyear climatology of DIN, DIP and chlorophyll *a* concentrations at station 330 in the BCS (1991–2010, monthly data). The vertical lines illustrate the multiyear P10–P90 range.

maximum. To take the losses into account, a regression can be made each year between the chlorophyll *a* maximum concentration and the 'effective' nutrients plotted at different locations (Fig. 2b). The inverse slope of the correlation gives the nutrient requirement necessary for the bloom formation. This nutrient requirement includes all the losses from phytoplankton during the growth period: the higher the losses, the higher the nutrient requirements. Some spatial and interannual variability is expected in this slope due to the variability in the losses or in the C:Chl ratio, reflecting the phytoplankton species assemblage. In our dataset, a larger variability is observed when comparing different years than when comparing different stations. The alternance in species dominance between *Phaeocystis* and diatoms in the spring bloom may also potentially introduce some variability, as a strong dominance of *Phaeocystis* could lower the DIP requirement for the bloom formation due to its affinity for organic phosphorus. The ensemble of yearly slopes could be summarized by a multiyear median value and a measure of the expected variability around this median.

2.2. Dynamics of nutrient conversion into biomass

The climatology of chlorophyll *a* and nutrients at station 330 in the BCS (Fig. 3) illustrates the conversion of winter nutrients into chlorophyll *a* during the spring biomass bloom.

In order to aid in the interpretation of the correlation '*Chlmax* vs. nutrients', a simpler approach is developed here to relate *Chlmax* to nutrient consumption, and to describe in simple terms the dynamics of chlorophyll *a* accumulation and losses during the spring bloom growth period. During the finite duration of the bloom, from initial growth at $t = 0$ to the biomass maximum at $t = t_m$, the phytoplankton biomass, B, is assumed vertically homogeneous and is expressed in nutrient units as follows:

$$\frac{dB}{dt} = \alpha B - \beta B \tag{1}$$

where growth processes are represented by the rate parameter, α, and all loss processes (mortality by predation/autolysis, settling), are represented by the rate parameter, β. Here, α and β (having dimension [time^{-1}]) are assumed constant in time in the spring growth period. This is, of course, an approximation as loss and growth process rates vary in this period. Assuming that all mortality is lost to the system, at least at short time scales, then the limiting nutrient, $Nut^{\lim}$, is simply depleted by conversion into phytoplankton biomass:

$$\frac{dNut^{\lim}}{dt} = -\alpha B \tag{2}$$

Initial conditions are:

$$\left.\begin{array}{l} B = B_0 \\ Nut^{\lim} = Nut_0^{\lim} \end{array}\right\} t = 0 \tag{3}$$

Final conditions are given at the peak of the biomass bloom, when $Nut^{\lim}$ is very low and B reaches a maximum, B_m (unknown):

$$\left.\begin{array}{l} B = B_m \\ Nut^{\lim} = Nut_m^{\lim} \end{array}\right\} t = t_m \tag{4}$$

The evolution equations for $Nut^{\lim}$ can be solved with these initial and final conditions.

$$Nut^{\lim} = Nut_0^{\lim} + \frac{\alpha B_0}{(\alpha-\beta)}\left(1 - e^{(\alpha-\beta)t}\right) \tag{5}$$

Applying the condition (4) that the bloom starts to decay when nutrients have very low concentrations sets the finish time or maximum bloom timing, t_m:

$$t_m = \frac{1}{(\alpha-\beta)} \ln_e \left[\frac{\left(Nut_0^{\lim} - Nut_m^{\lim}\right)}{B_0}\frac{(\alpha-\beta)}{\alpha} + 1\right] \tag{6}$$

It is seen that the loss processes will also affect the timing of the peak of the bloom, which is significantly delayed if β is large compared to α. Finally, the phytoplankton biomass increase is given by:

$$B_m - B_0 = \left(Nut_0^{\lim} - Nut_m^{\lim}\right)\left(1 - \frac{\beta}{\alpha}\right) \tag{7}$$

This has the simple extreme case that when $\beta = 0$, then B_m - $B_0 = Nut_0^{\lim} - Nut_m^{\lim}$ i.e. if there are no losses then dissolved nutrients are converted 100% into phytoplankton biomass. The other extreme case is when $\beta = \alpha$ and $B_m = B_0$, i.e. zero growth. In intermediate cases, and assuming that the limiting nutrient is almost depleted at the spring bloom peak, Eq. (7) gives:

$$B_m \approx \kappa Nut_0^{\lim} \tag{8}$$

where $\kappa = 1 - \beta/\alpha$ is a dimensionless factor, between 0 and 1, representing the "efficiency of nutrient conversion" into phytoplankton biomass. The above-made approximation that α and β are assumed constant over the growth period becomes less important when considering the β/α ratio.

2.3. Correlations between chlorophyll a, nutrients and salinity

The correlation between the chlorophyll *a* spring maximum, *Chlmax*, and the winter nutrients has first been tested with the results of a biogeochemical model (3D-MIRO&CO), and secondly with field observations from the North Sea continental shelf (see Sections 2.5, 2.6 and 2.7 for a description of the model and the datasets). The analysis consists in applying two simple linear relationships: one linking winter nutrients (*Nutwi*) to winter salinity (*Salwi*), and another one linking *Chlmax* to the 'effective' nutrient concentration (*Nuteff*, see Fig. 2). The first linear regression links nutrient concentrations to salinity at the end of the winter.

$$Nutwi = a * Salwi + b \tag{9}$$

where the regression slope and offset, *a* and *b*, may vary from year to year. In coastal areas, this relationship is expected to be strong as the pre-bloom nutrient levels are mainly enriched by continental freshwater discharge (see also the statistical model in De Vries et al., 1998). In offshore areas, salinity variations are linked to oceanic inputs and to the mixing with remote river plumes (Lacroix et al., 2004). Though salinity variations are relatively lower offshore than in the coastal zone, the relationship between nutrients and salinity should hold also in offshore areas, provided that there is conservative mixing of essentially only two distinct water masses, oceanic and freshwater (two "end-members" to a dilution line).

Prior to the second regression, which links *Chlmax* to *Nuteff*, the 'effective' nutrients are estimated by applying two corrections on *Nutwi*. Advection between winter and spring is accounted for by knowing salinity variations between winter and spring, and by using each year the coefficients from Eq. (9). For location i and year j:

$$Nuttran_{ij} = Nutwi_{ij} + \left(Salpeak_{ij} - Salwi_{ij}\right) * a_j \tag{10}$$

where $Nuttran_{ij}$ is the 'transported' nutrient concentration, i.e. corrected for the advection, $Salpeak_{ij}$ is the salinity at the moment of *Chlmax*, and a_j is the slope in Eq. (9) for year *j*. The remaining nutrients at the peak (*Nutpeak*) are subtracted from the 'transported' nutrients to get *Nuteff*:

$$Nuteff = Nuttran - Nutpeak. \quad (11)$$

The linear regression between *Chlmax* and *Nuteff* reads:

$$Chlmax = m * Nuteff + p. \quad (12)$$

This equation is similar to Eq. (8) and, assuming $p \approx 0$, it reads:

$$Chlmax \approx (1-\beta/\alpha)\ \xi\ Nuteff = \xi\ \kappa\, Nuteff \quad (13)$$

where ξ is a constant factor with dimension [gChl mol-nutrient^{-1}] representing the "chlorophyll-to-nutrient cellular ratio" of phytoplankton. In the 3D-MIRO&CO model, the internal nutrient ratios for phytoplankton are $\xi^N = 1.968$ gChl molN^{-1} and $\xi^P = 31.2$ gChl molP^{-1} (derived from Lancelot et al., 2005). It should be pointed out that, in Eq. (13), both DIN or DIP may be used, whether they are limiting or not, as long as the second correction is applied (Eq. (11)). The factor $(\xi \cdot \kappa)^{-1}$ is the "spring-bloom nutrient requirement" or the nutrient concentration necessary at the end of the winter to form one unit of chlorophyll *a* at the spring bloom peak, all losses included.

Any given year, the ratio between nutrient requirements gives the DIN-to-DIP requirement for the bloom formation. This requirement compared to measured winter DIN:DIP ratios enables prediction of which nutrient will be limiting at any salinity.

2.4. Rebuilding Chlmax from salinity

Once the winter nutrient dilution rates and the nutrient requirements are established, the *Chlmax* may be estimated from salinity. This requires to apply the two corrections to get *Nuteff* from *Nutwi* (Eqs. (10) and (11)). The spring salinity must be known, and the remaining nutrient at the peak must be known. When spring salinity is not known, e.g. when predicting *Chlmax* in winter, the prediction is made with winter salinity. Then, the resulting *Chlmax* is assumed identical for the same spring salinity, wherever it is found one month later. The second condition simplifies when considering the limiting nutrient, and assuming that its remaining concentration is negligible at the moment of *Chlmax*.

2.5. Description of the 3D-MIRO&CO model

The 3D-MIRO&CO model (Lacroix et al., 2007b) is a three dimensional numerical model, coupling the hydrodynamical model COHERENS (Luyten et al., 1999) and the biological model MIRO (Lancelot et al., 2005), to describe the biogeochemical and ecological dynamics in the Southern North Sea. The model domain covers the English Channel and the Southern Bight of the North Sea (latitude: 48.5°N to 52.5°N, and longitude: 4°W to 4.5°E). A validation of this model was presented previously for salinity (Lacroix et al., 2004) and for nutrients and chlorophyll *a* in Lacroix et al. (2007b). The only differences between the previous version of the model and the present one are that:

1— the light attenuation is determined from a daily TSM climatology derived from remote sensing observations over four years (2003–2006) and gap-filled with DINEOF method (Sirjacobs et al., 2011), instead of from seasonal time series;
2— a re-calibration of the minimum specific rates of phytoplankton cellular autolysis has been performed (natural mortality; see Lancelot et al., 2005);
3— the phytoplankton production is suppressed in the Westerschelde part of the model by artificially increasing the TSM concentration. Phytoplankton production is naturally low there due to a combination of bathymetry and turbidity, both of which cannot be adequately represented at relevant spatial resolution for the estuary in the present model;
4— the seasonal concentration of phytoplankton species imposed at the Western boundary of the model is corrected with respect to Lacroix et al. (2007b).

The first correction introduces a more realistic TSM forcing from remote sensing observations (MODIS TSM climatology between 2003 and 2006). The issue of cloud coverage masking the observation has been solved with the gapfilling technique DINEOF (Sirjacobs et al., 2011) providing one data per day in every pixel. This TSM forcing is used in the calculation of the light penetration into the water column. As a consequence of this improvement to the model, a delay was observed in the timing of the chlorophyll *a* spring peak by minimum ten days, when compared to the previous model version. The second correction, the re-calibration of the minimum specific rate of cellular autolysis, cancels the delay in the timing of the phytoplankton spring bloom. It consists in lowering the values of phytoplankton autolysis coefficients by 90% for spring diatoms, by 50% for summer diatoms and for nanoflagellates. Regarding *Phaeocystis*, the colonial lysis parameter has been kept intact in the model as it is the main cause of *Phaeocystis* mortality after the spring bloom (Brussaard et al., 1995), but the cellular autolysis was canceled in the model. This correction is supported by a sensitivity study showing the influence of the cellular autolysis on the timing and the intensity of the phytoplankton spring bloom. As opposed to other parameters in the 3D-MIRO&CO model, the phytoplankton lysis was not directly measured for the Belgian phytoplankton species, but adapted from values found in the Marsdiep area (Lancelot et al., 2005, see Brussaard et al., 1995). The phytoplankton growth and loss fluxes during the spring bloom period, calculated at the Belgian station 330 (see Fig. 1), have been modified by this parameter re-calibration. The loss-to-growth ratio decreased from 50% to 40% during the blooming period compared to before the re-calibration in the simulated year 2000. The re-calibration of the autolysis parameter alone allowed improving considerably the model performances in reproducing the phytoplankton bloom timing and intensity, and the time series of nutrient concentrations. The third correction drastically decreases the chlorophyll *a* concentrations in the Westerschelde (which were previously significantly overestimated) and, hence, allows for a more realistic export of dissolved nutrients into the coastal zone during the growth season. The fourth correction, regarding the phytoplankton concentration at the Western boundary, has been made on the basis of field observations (SOMLIT). A climatology (2000–2008) of monthly chlorophyll *a* concentration has been built from data collected at the station "Roscoff Astan" (data provided by the "Service d'Observation en Milieu Littoral", INSU-CNRS, Roscoff). These chlorophyll *a* data have been converted into carbon biomass, and distributed between the species which are included in the model as state variables, i.e. diatoms (80% of phytoplankton carbon biomass), *Phaeocystis* colonies (10%), and nanoflagellates (10%). Also, each species biomass has been subdivided into the three modeled internal compartments of phytoplankton: functional (F, 80% of phytoplankton carbon, which also corresponds to 100% of the chlorophyll *a*), substrates (S, 6% of phytoplankton carbon) and reserves (R, 14% of phytoplankton carbon). These modifications improve the modeled phytoplankton production and biomass close to the Western boundary.

2.6. Model results used in the correlations

The correlations between *Chlmax* and nutrients explained above in Sections 2.1, 2.2 and 2.3 have first been tested with results from the 3D-MIRO&CO model. A series of successive runs have been made from the year 1991 to 2006, each year starting with the ending conditions of the previous year. The initial conditions in 1991 have been generated by repeating the forcings of 1991 during a spin-up run of three years. To perform the correlations in this study, model results have been taken in

three different years showing contrasted meteorological conditions, i.e. 1998 (dry year), 2000 (average conditions), and 2001 (wet year). In 1998, a lower than average rainfall over northwest Europe combined with a higher than average Atlantic water penetration through the English Channel resulted in an overall high salinity within the BCS, with the dispersion of freshwater confined into a small area close to the coast. On the contrary, in 2001, high rainfall combined with a lower than average Atlantic penetration in the BCS resulted in an extended area of low salinities across the domain, with a high offshore dispersion of freshwater. Considering contrasted years allowed estimating some interannual variability through the 3D-model simulations.

2.7. In situ data used in the correlations

Several datasets have been used to reproduce the '*Chlmax* vs. nutrients' regressions made with model results. The first dataset includes surface salinity, dissolved nutrients and chlorophyll *a* concentrations at twenty-three stations in the BCS for the period 1991–2010 (national monitoring program; Belgian Marine Data Centre, www.bmdc.be). The second dataset includes similar data at fifty stations in the DCS for the period 1976 to 1990 and at twenty stations in the DCS for the period 1991 to 2010 (national monitoring program of the Dutch Rijkswaterstaat, http://live.waterbase.nl; see Baretta-Bekker et al., 2009; Prins et al., 2012). The third dataset holds continuous ODAS-FerryBox (ODAS-FB) recordings of surface salinity and chlorophyll *a* fluorescence in the BCS during the RV Belgica cruise of 21st to 25th April 2008. In both the BCS and the DCS, surface concentrations of salinity, dissolved nutrients and chlorophyll *a* are assumed to reflect the concentrations in the whole water column due to good vertical mixing in the period between February and April. Regarding the two national monitoring programs, monthly averages were considered. In many cases, a maximum of one sample per month and per sampling station was available, and many gaps were found in the data.

In order to draw the correlations, the following data are needed every year in several stations: the winter salinity and nutrients (N, P), and the spring salinity, nutrients and chlorophyll *a* at the moment of the spring bloom. This set of values had to be found in each station for the data to be considered in the '*Chlmax* vs. *effective nutrients*' correlation (see Fig. 2). A minimum number of four stations each year were estimated necessary to draw reasonable correlations over the salinity range (most years show about ten stations). Finally, the removal of very bad correlations ($R^2 < 0.4$), due supposedly to sampling uncertainties like the 'post-bloom case' (see Section 2.8), led to a decrease of exploitable data.

The resulting collection of slopes (~4 to 8 elements) is non-normally distributed due to the impact of extreme years. A multiyear median value is assumed to represent the central tendency in the '*Chlmax* vs. *effective nutrients*' regression slopes. In the present study, the limited size of exploitable in situ data may seem improper to perform any statistics on the interannual uncertainty in the '*Chlmax* vs. *effective nutrients*' regression slopes. Instead we estimate the measure of expected variability (i.e. mev) around the median for *n* years as:

$$\mathrm{mev} = \frac{1}{n}\sqrt{\sum_{i=1}^{n}(x_i - \mathrm{median})^2} \tag{14}$$

where x_i is the regression slope of one year. The coefficient of variation in this study is the ratio between the mev and the median.

2.8. Definitions of winter and spring maximum parameters

In the North Sea continental waters, the phytoplankton bloom starts on average around mid-February or the beginning of March, and reaches the peak around mid-April (Rousseau et al., 2006, see also Fig. 3). In the model, the period of the bloom formation is therefore defined between the end of February (i.e. day 60) and the day of the chlorophyll *a* spring maximum. The "winter" nutrient concentrations and salinity are considered on day 60. The "spring peak" concentrations in nutrients, and the "spring peak" salinity, are given by their respective values on the chlorophyll *a* spring maximum at each location. The selection is made for each grid cell individually, as the day of spring maximum may vary slightly from one grid cell to the other in a given year.

Regarding the field observations of salinity, nutrient and chlorophyll *a* concentrations the definitions of "winter" and "spring peak" values are slightly different due to the discontinuity in the available time series of data. Most years only one value is available in January or February, and an average between the two months was used as an estimate of the "winter" mean – or pre-bloom level – for nutrients and salinity. Maximum values of chlorophyll *a* were used as a proxy for the spring-bloom maximum biomass of phytoplankton. The timing of the chlorophyll *a* maximum (April or May) was detected with a simple algorithm. Most of the time, the chlorophyll *a* spring maximum occurred in April. Corresponding values of nutrient concentration and salinity were used as "spring peak" values. Though the available chlorophyll *a* data offer a good picture of the seasonal trends in the North Sea continental waters, monthly data do not capture the high-frequency dynamics of the phytoplankton spring bloom and it is noted that some variations may be characterized at time scales as short as 5 to 10 days (see e.g. Mieruch et al., 2010). Whereas the chlorophyll *a* values in the data almost always present a maximum in April, the values sampled in April do not necessarily correspond to the real bloom maximum occurring in the natural system. Therefore, any study regarding the bloom maximum made with monthly data includes an under-sampling uncertainty, and this uncertainty biases towards an underestimate of the real bloom maximum. In addition, if the April samples of nutrients and chlorophyll *a* are collected after the bloom peak occurred (i.e. the post-bloom case), then the underlying assumptions leading to Eq. (7) plus the assumption that

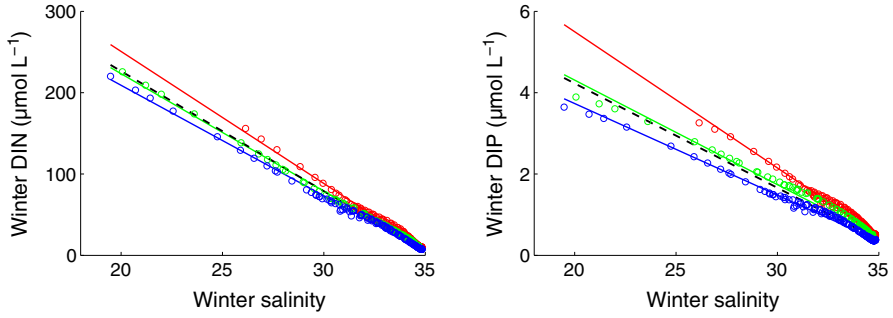

Fig. 4. Results from the 3D-MIRO&CO model in the BCS and the Scheldt estuary. Mixing diagrams of winter DIN and winter DIP against winter salinity for three years showing contrasted meteorological conditions: 1998 (dry, red), 2000 (avg, green), and 2001 (wet, blue). Every dot represents the winter value in one grid cell in the BCS. Yearly and multiyear-median (dashed black) regressions are shown; see Table 1 for values.

spring-peak nutrient concentrations represent the remaining nutrients at the time of *Chlmax* are no longer valid. In the present study, it was not possible to distinguish the post-bloom cases.

3. Results

3.1. Mixing diagrams for DIN and DIP

In 3D-MIRO&CO results, there is a strong linear relation between winter salinity and both winter DIN and DIP in the BCS with some interannual variations (Fig. 4). As limited biological processes take place in winter, the model nutrient dilution rates (i.e. the slopes of the regressions) are almost linear. The interannual variability is especially visible at the upstream end-member of the Scheldt estuary, while the downstream oceanic end-member shows much less variability for salinity >34 psu. The interannual variability at the upstream end-member is explained by rainfall, and more specifically by the combination of two processes: nutrient emissions from the watershed to the estuary and dilution of concentrations by freshwater in the estuary. In the Scheldt basin, the DIN emission from the watershed to the river increases slightly with rainfall as a consequence of fertilizer leaching, whereas the DIP emission is less affected by rainfall (Brion et al., 2006).

Mixing diagrams of winter nutrients against winter salinity have also been drawn from in situ observations made between 1991 and 2010 in the BCS and between 1976 and 2010 in the DCS (Fig. 5). The data in the DCS have been separated into two different periods, i.e. 1976–1990 and 1991–2010. This is due to the considerable decrease in DIP emissions to the sea ca. 1990 (see De Vries et al., 1998 for comparable slopes of nutrients vs. salinity in the DCS). The response of the dilution lines to decreased emissions is visible, and the linearity of the dilution is conserved after 1990. The period 1991–2010 is also suitable for comparison between the Belgian and Dutch datasets. A pronounced interannual variability in winter salinity and in winter nutrient concentrations is illustrated by the 10- and 90-percentile lines. The interannual variability in the winter nutrient dilution rates (Fig. 6) suggests that the variations due to dry and wet years are superimposed for DIP on a historical decreasing trend resulting from the efforts in wastewater treatment (see e.g. De Vries et al., 1998 and Soetaert et al., 2006). The characteristics of the multiyear dilution lines shown in Figs. 4 and 5 for model results and field data are compared in Table 1.

In the BCS, the winter mean dilution rates for DIN and DIP are very comparable between model results and in situ observations. In the period 1991–2010, the dilution rates observed in the DCS show lower slope values than in the BCS for both nutrients as the upstream end-members are different. Nutrients are slightly more concentrated in the Scheldt than in the Rhine/Meuse system. Yet, the freshwater discharge in the Scheldt is considerably lower than in the Rhine (a factor 20; Wollast, 2003), resulting in less nutrient loadings to the sea at the Scheldt mouth.

3.2. 'Chlmax vs. nutrient' relationship

In 3D-MIRO&CO, the correlation between *Chlmax* and winter nutrients in the BCS is weak in the test years 1998, 2000 and 2001 (Fig. 7). The same holds for the correlation between *Chlmax* and winter salinity. However, the correlation improves when plotting *Chlmax* vs. spring peak salinity (i.e. the salinity at the moment of *Chlmax*), though not for salinities lower than 30 due to the light-limitation of phytoplankton production in the Scheldt estuary or its plume in the coastal zone. Taking spring peak salinity into account and applying the correction for advection on winter nutrients (Fig. 2, Eq. (10)) also increases the correlation '*Chlmax* vs. transported nutrients'. When applying the second correction for the remaining nutrients at the peak thus getting the effective nutrients, *Nuteff* (see Eq. (11)), the correlation '*Chlmax* vs. *Nuteff*' improves considerably and a multiyear regression line can be drawn (see Table 2). The slope of '*Chlmax* vs. *DINeff*' has obviously increased due to the second correction, suggesting that DIN is not depleted at the chlorophyll *a* spring peak, at least in high biomass areas, and indicating a potential P-limitation of phytoplankton production (see Section 3.4).

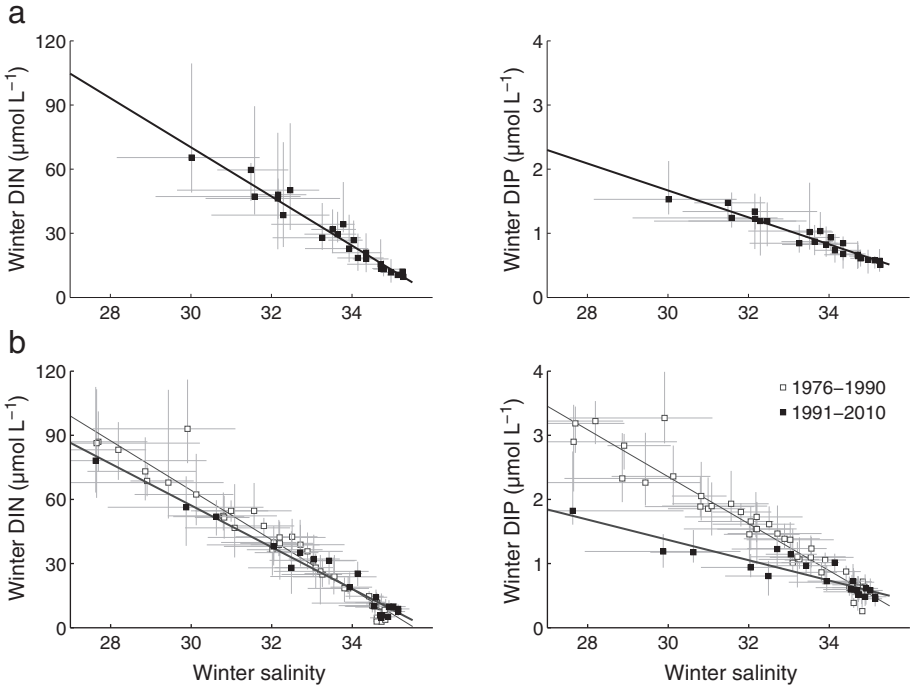

Fig. 5. In situ data. (a) Mixing diagrams of winter nutrients against winter salinity at 23 stations in the BCS during the period 1991 to 2010. Each square represents the median of winter values at one station. Gray lines scale the interannual variability (10 and 90 percentile) in salinity (horizontal) and in nutrients (vertical) at each station over the period. See Table 1 for slope values of black regression lines. (b) Mixing diagrams of winter nutrients against winter salinity in the DCS. Because of the significant reduction in P emissions circa year 1990, and to remain consistent with regard to the Belgian dataset, two periods are distinguished: 1976–1990 (covering 50 stations) and 1991–2010 (covering 20 stations).

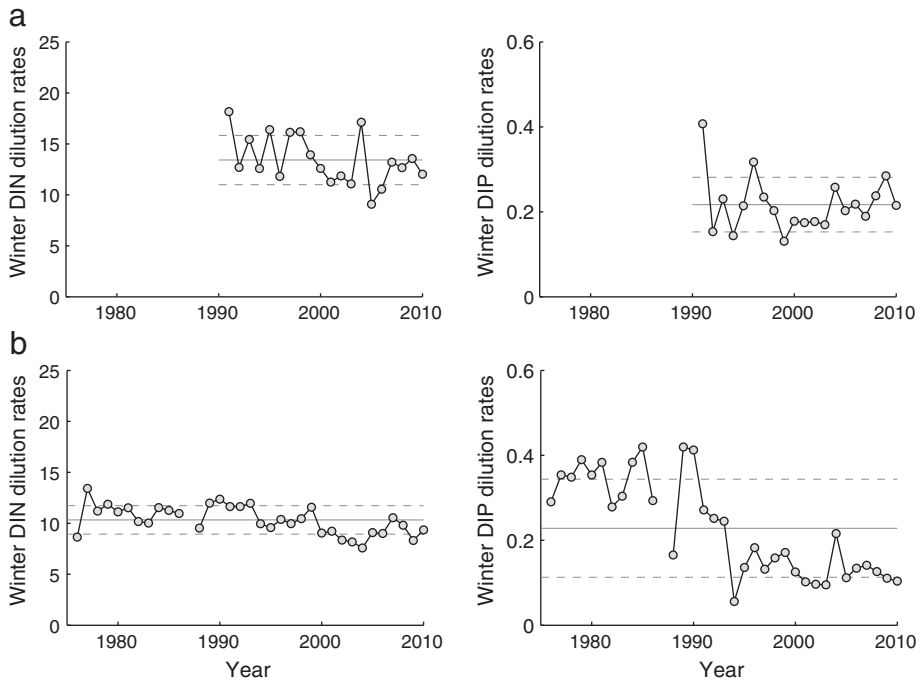

Fig. 6. In situ data. (a) Interannual variability of the winter dilution rate of DIN and DIP in the BCS between 1991 and 2010. The mean values (horizontal lines) and the standard deviations (dashed lines) over the period are drawn. Dilution rates (μmol L^{-1} psu^{-1}) are the regression slopes of the mixing diagrams "winter nutrients vs. winter salinity". (b) Interannual variability of the winter dilution rate of DIN and DIP in the DCS between 1976 and 2010.

The multiyear regression line of '*Chlmax* vs. *Nuteff*' may be used to rebuild the chlorophyll *a* spring maximum from nutrients (according to the method proposed in Section 2.4). In Fig. 8, the winter DIP is first rebuilt from winter salinity, then *Chlmax* is rebuilt from *DIPeff* after the appropriate corrections. The rebuilt *Chlmax* compares fairly well with the reference *Chlmax* in the 3D-MIRO&CO model, as illustrated in Figs. 8 and 9.

The correlations between *Chlmax* and nutrients have also been drawn with in situ observations made between 1991 and 2010 in the BCS and the DCS. The yearly slope values for DIN and for DIP are shown in Fig. 10, and a multiyear median value is calculated (see also Table 2). In the natural system, the relationship between *Chlmax* and nutrients shows more interannual variability than in the model results. The coefficients of variation are globally lower in the DCS than in the BCS. This may be due to the smaller number of data in the DCS, linked to the relative lack of exploitable data. In both the DCS and the BCS, the coefficients of variation are lower when correlating *Chlmax* with *DIPeff* than with *DINeff*, indicating that DIP would be a more reliable predictor of *Chlmax* in the North Sea continental waters.

When dividing the yearly slopes to get the yearly DIN-to-DIP requirements (Fig. 10, bottom graphs), a multiyear median value of 34.4 molN $molP^{-1}$ is obtained in the BCS compared to 28.6 molN $molP^{-1}$ in the DCS, with similar coefficients of variation. In the BCS, the values of DIN-to-DIP requirement are not very dispersed from year to year, except in the year 1991 when an exceptionally high value was found. It has been shown that the year 1991 exhibited very high concentrations in *Phaeocystis* spp., and a high *Phaeocystis*/diatom ratio during the spring bloom (Breton et al., 2006). Independently of other causes of variability, a strong dominance of *Phaeocystis* over diatoms in the spring would theoretically correspond to high DIN-to-DIP requirements during the spring biomass bloom formation. The affinity of *Phaeocystis* for organic phosphorus causes the colonies to potentially grow under very low DIP concentrations. A significant increase in *Chlmax* on another source than DIP will result in a relative increase of the slope '*Chlmax* vs. *DIPeff*', not to be found in the slope '*Chlmax* vs. *DINeff*'. As a result, the DIN-to-DIP requirement should increase.

Similar to what was done with the model results, the nutrient requirements obtained from in situ data may be used to rebuild *Chlmax* (Fig. 11). The continuous observations of salinity from the ODAS-FB during a RV Belgica cruise in April 2008 in the BCS have been converted into a rebuilt spring DIP, which in turn was converted into a rebuilt *Chlmax*. This rebuilt *Chlmax* may be compared with the fluorescence measured simultaneously by the FB (in chlorophyll *a* units).

The ODAS-FB data contain in situ information covering a large spatial range at a given time. A scatter plot of the ODAS-FB fluorescence against salinity in April 2008 during the cruise (Fig. 12A) confirms the general correlation between these two parameters, except in the Scheldt estuary where phytoplankton production is light-limited (sal < 30). When drawing a scatter plot with the rebuilt *Chlmax* obtained in Fig. 11 versus the ODAS-FB fluorescence in Fig. 11, a good correlation is obtained (Fig. 12B; $R^2 = 0.78$) in spite of the uncertainty in converting in situ fluorescence into chlorophyll *a*. Rebuilt *Chlmax* can result from DIP or from DIN. When rebuilt from DIN, *Chlmax* is clearly above the 1:1 line especially at high chlorophyll *a* values, i.e. in the coastal zone. Conversely, at low chlorophyll *a* values, i.e. offshore, the rebuilt *Chlmax* from DIP appears above the 1:1 line. Here, the nutrients remaining in April have not been subtracted from the rebuilt DIP and DIN to get *DIPeff* and *DINeff*, because they were not continuously measured by ODAS-

Table 1
Statistics on the regressions of dilution lines for end-of-winter nutrients in the BCS and the DCS (only multiyear median regressions).

Dilution lines: winter nutrients vs winter salinity						
	Slope (μmol L^{-1} psu^{-1})		Offset (μmol L^{-1})		R^2	
	DIN	DIP	DIN	DIP	DIN	DIP
Model results BCS (1998, 2000, 2001) Fig. 4	−13.9	−0.270	493	9.88	0.97	0.88
In situ obs. BCS (1991–2010) Fig. 5a	−11.5	−0.210	415	7.97	0.95	0.93
In situ obs. DCS (1976–1990) Fig. 5b	−11.6	−0.366	412	13.3	0.96	0.94
In situ obs. DCS (1991–2010) Fig. 5b	−9.76	−0.158	350	6.12	0.96	0.83

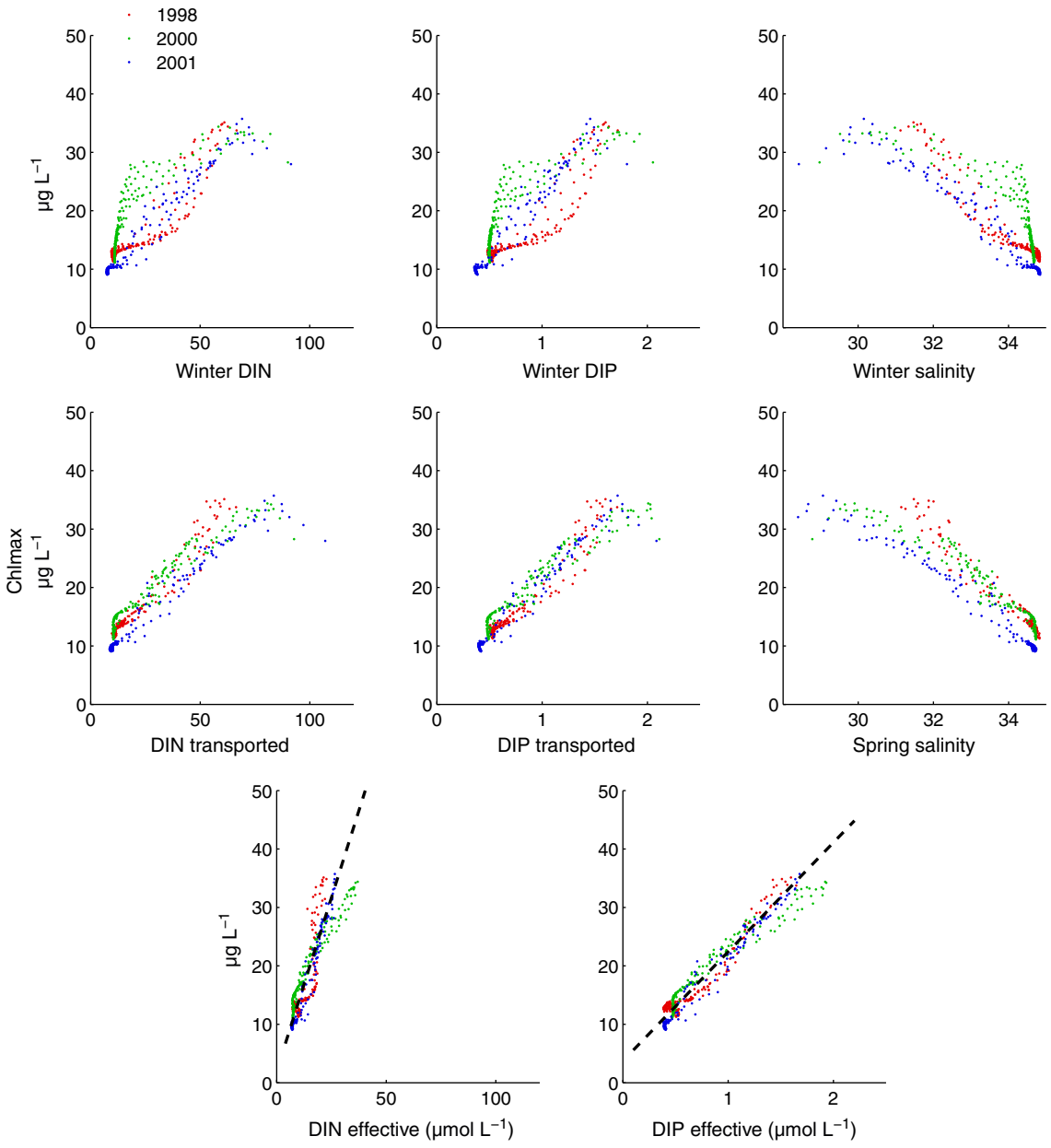

Fig. 7. Results from 3D-MIRO&CO model in the BCS (excluding the Scheldt estuary). Correlations between *Chlmax* and nutrients and between *Chlmax* and salinity for three years showing contrasted meteorological conditions (1998, 2000 and 2001). Top: End-of-winter nutrient concentrations (day 60) are neither corrected for transport nor for the remaining nutrients at the peak. Middle: Nutrient concentrations are corrected for transport only. Bottom: Nutrient concentrations are corrected for both transport and remaining nutrients at the peak. The dashed line is the multiyear median of regression lines (see corresponding statistical values in Table 2).

FB. In Fig. 12B, it can be assumed that the distance from the 1:1 line is mainly due to the lack of this nutrient correction. To confirm this idea, a similar graph with much less data is drawn but only at the sampling stations where nutrients and chlorophyll *a* (HPLC) have been measured during the same campaign (Fig. 12C). There, the necessary corrections could be done, and the gaps to the 1:1 line have been reduced at both low and high rebuilt chlorophyll *a* values. The effect of the second correction implies that in April DIN remains relatively in excess in the

Table 2
Statistics on the multiyear regression lines *Chlmax* vs. 'effective' nutrients in the BCS and the DCS (model results and in situ data). The R^2 values for in situ data in the BCS and the DCS are the lowest and highest yearly R^2 values. These values illustrate the spatial correlations between stations on a given year.

Nutrient conversion: *Chlmax* vs 'effective' nutrients							
		Slope (µgChl µmol^{-1})		Offset (µgChl L^{-1})		R^2	
		DIN	DIP	DIN	DIP	DIN	DIP
Model results BCS Fig. 7	Multiyear median	0.934	17.4	4.98	4.40	0.82	0.94
In situ obs. BCS Fig. 10A	Multiyear median	0.608	36.6	−1.46	−4.40	0.49 to 0.93	0.46 to 0.98
In situ obs. DCS Fig. 10B	Multiyear median	1.24	40.0	−3.17	−8.56	0.76 to 0.93	0.72 to 0.94

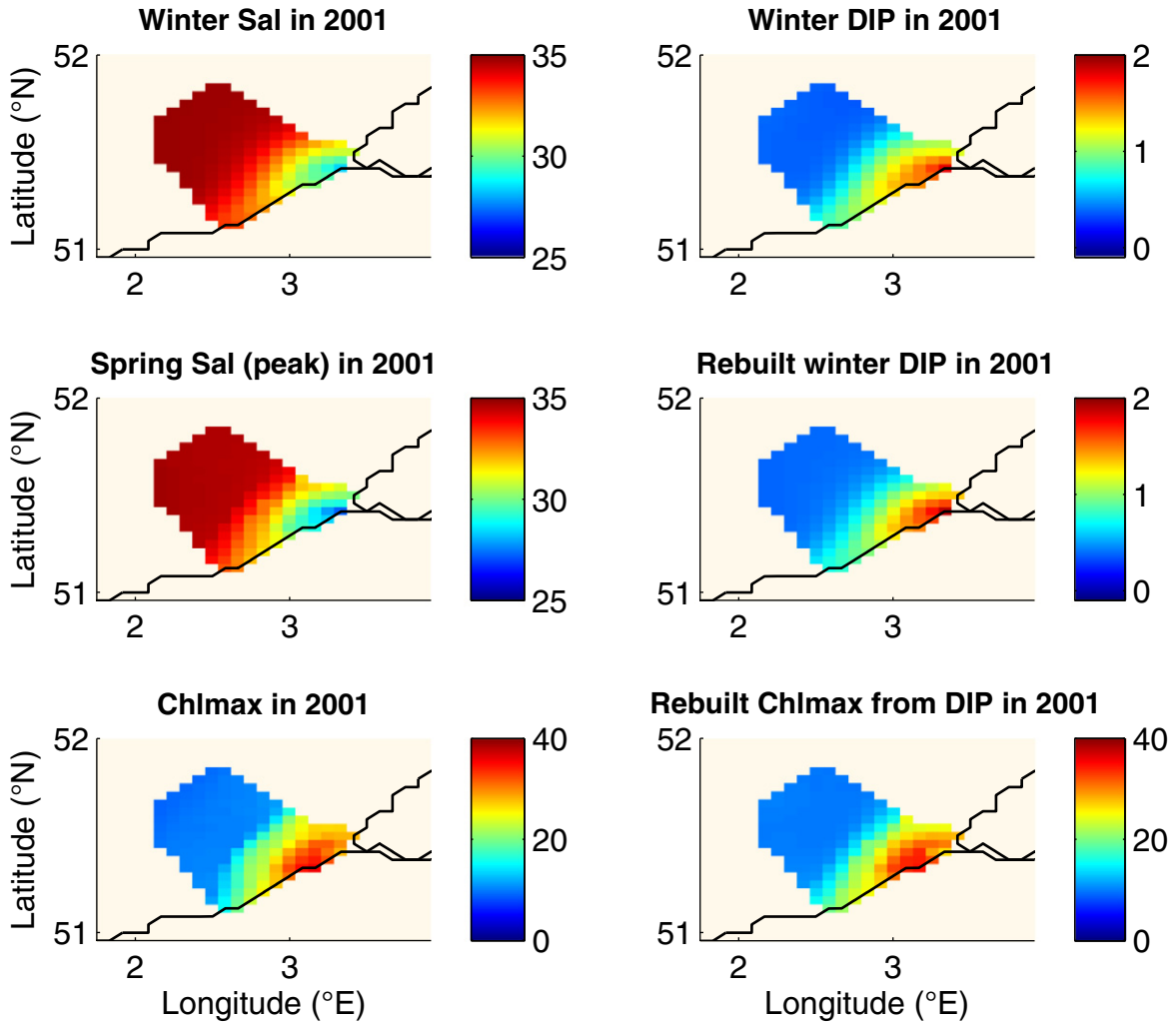

Fig. 8. Steps of *Chlmax* rebuilding from salinity with 3D-MIRO&CO model results in the BCS in the year 2001. Top — Winter salinity, and reference winter DIP as output from 3D-MIRO&CO simulation. Middle — Spring salinity as given by 3D-MIRO&CO (at *Chlmax* timing), and rebuilt winter DIP by winter salinity. Bottom — Reference *Chlmax* as given by 3D-MIRO&CO, and rebuilt *Chlmax* predicted from rebuilt winter DIP, after the correction for advection using the difference between winter salinity and spring salinity and subtraction of remaining DIP at the peak.

coastal zone while DIP is very low, and it is the opposite offshore. This suggests that a switch from a P-limitation to a N-limitation occurs along the transect coastal-offshore in April 2008 (see Section 3.4). In order to predict *Chlmax* from salinity when the nutrient requirements are unknown, e.g. in winter for the coming spring biomass bloom, the interannual median of the nutrient requirement may be used by default (Fig. 10, Table 2). In Fig. 12D, the *Chlmax* is rebuilt from DIN and DIP (just as in Fig. 12B) using the interannual median of nutrient requirements instead of the values in 2008. When rebuilt from DIP, the *Chlmax* is quite similar in both figures because the median and the 2008 values of the DIP requirement are very close. However, the DIN requirement in 2008 was quite far from the interannual median value and, hence, the *Chlmax* rebuilt from DIN is significantly lower in Fig. 12D than in Fig. 12B. The fact that the DIP requirement exhibits lower interannual variability than the DIN requirement advocates for choosing the median DIP requirement to rebuild *Chlmax* by default. Still, any such prediction would be accompanied by a variability of 12%, and of about 35% for extreme years. The measure of the expected variability could be improved through a broader analysis with larger datasets.

3.3. Nutrient requirements and internal nutrient ratios

The regression slopes for '*Chlmax* vs. *DINeff*' in the BCS and the DCS differ by a factor two (Table 2), while the regression slopes for '*Chlmax*

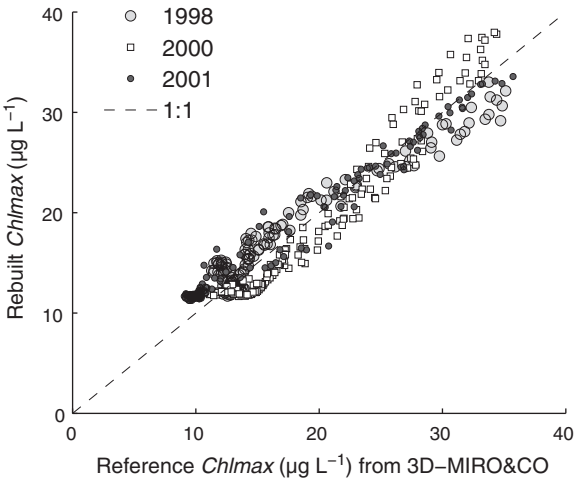

Fig. 9. Correlation ($R^2 = 0.93$) established between rebuilt *Chlmax* (from rebuilt DIP) and reference *Chlmax* output from 3D-MIRO&CO in every grid cell of the BCS for three different simulated years.

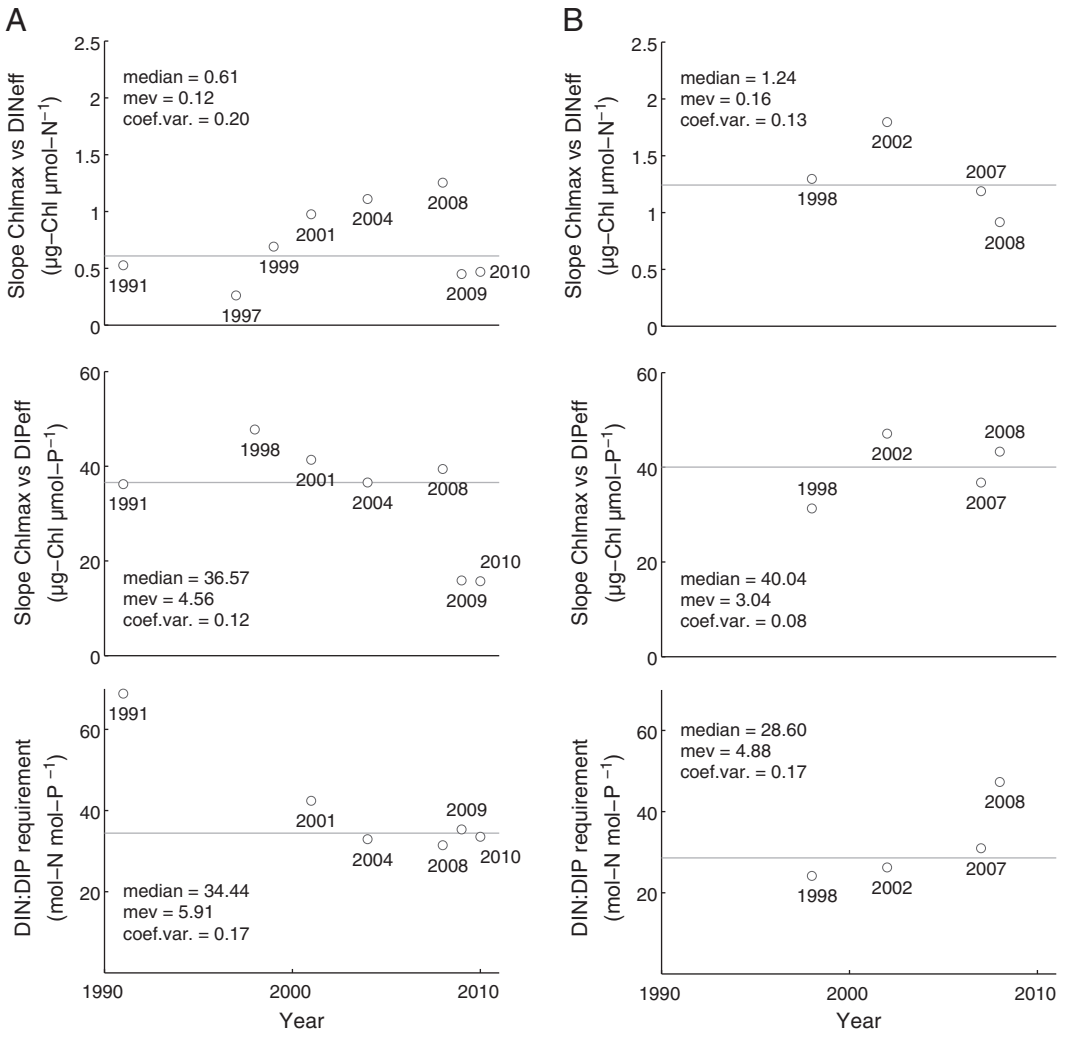

Fig. 10. In situ data. (A) Top and mid: yearly regression slopes between *Chlmax* and 'effective' nutrients in the BCS for some years between 1991 and 2010. Bottom: yearly DIN-to-DIP requirement for *Chlmax* formation in the BCS. The horizontal line represents the multiyear median. (B) Yearly regression slopes between *Chlmax* and 'effective' nutrients in the DCS for some years between 1991 and 2010. Values for the multiyear median, the measure of expected variability around the median (mev), and the coefficient of variation are given in each plot (see also Tables 2 and 3).

vs. *DIPeff*' are of the same order. The DIN-to-DIP requirement obtained with in situ data in the BCS and the DCS show close values, and remarkably the value in the BCS is identical to the one derived from measurements on *Phaeocystis* chlorophyll *a* in 2003 by Muylaert et al. (2006) (see Table 3). As the DIN-to-DIP requirement is a property of the spring phytoplankton communities, the similarity between these values supports that the spring natural assemblage of phytoplankton is often dominated by *Phaeocystis* in this system.

To emphasize the difference between "nutrient requirements" and "nutrient cellular ratios" of phytoplankton, Table 3 also shows the constant Redfield ratios and the constant cellular ratios as imposed to the model 3D-MIRO&CO (estimated through laboratory measurements during the growth phase of phytoplankton; see Lancelot et al., 2005). The difference between cellular nutrient ratios of phytoplankton and nutrient requirements for phytoplankton spring bloom is due to the losses occurring during the bloom formation (see Eq. (13)). In the absence of losses (i.e. $\beta = 0$ and hence $\kappa = 1$), the nutrient requirements would be equal to the cellular ratios of phytoplankton.

3.4. Predicting the spring nutrient limitation

The above results in April 2008 suggested a P-limitation of the spring phytoplankton bloom in coastal areas and a N-limitation offshore. The low winter DIN:DIP ratios generally found offshore at sea tend to confirm a potential nitrogen limitation of the phytoplankton spring bloom in these areas. On the contrary, the continental coastal waters generally exhibit high winter DIN:DIP ratio and are thought to be potentially limited by P in the spring bloom. This reasoning does not give any accurate information about the switch in limitation between coastal and offshore areas. The evaluation of the spring nutrient limitation proposed in this study is more informative in this respect and may be done with in situ data only. The spring-bloom DIN-to-DIP requirement is calculated from the regressions '*Chlmax* vs. *Nuteff*' in the BCS and the DCS (Fig. 10 bottom; see multiyear median values in Table 3). When comparing the winter DIN:DIP ratio, varying in the salinity gradient, to the phytoplankton DIN-to-DIP requirement, constant in the salinity gradient, it is possible to predict which nutrient will limit *Chlmax* in the spring as a function of salinity (Fig. 13). The 3D-MIRO&CO model results in the BCS indicate that a switch takes place between a P- and a N-limitation at salinities 32.7 to 33.9 depending on the year. The in situ observations over the period 1991–2010 in the BCS and the DCS show similar trends in nutrient limitation. In spite of a slightly different DIN-to-DIP requirement, the BCS and the DCS waters are characterized by a switch in nutrient limitation occurring at similar salinities, i.e. 33.5 in the BCS and 33.6 in the DCS.

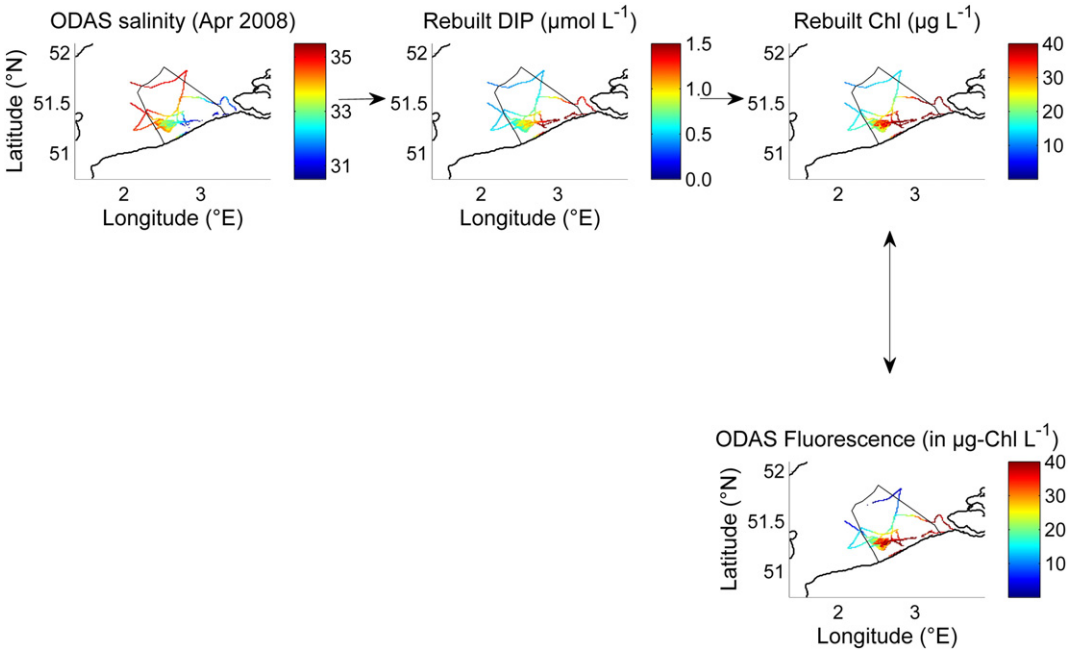

Fig. 11. Example of *Chlmax* rebuilding from in situ spring salinity, and comparison with in situ measured fluorescence (ODAS-FB in the BCS — 21st to 25th April 2008). Spring DIP is linearly rebuilt from spring salinity with the coefficients of the '*DIP* vs. *salinity*' regression made for the year 2008 in the BCS (slope = −0.270 µmol L^{-1} psu^{-1}; offset = 9.88 µmol L^{-1}). *Chlmax* is linearly rebuilt from rebuilt spring DIP with the coefficients of the '*Chlmax* vs. *DIPeff*' regression made for the year 2008 in the BCS (slope = 39.4 µgChl µmolP^{-1}; offset = −4.17 µgChl L^{-1}).

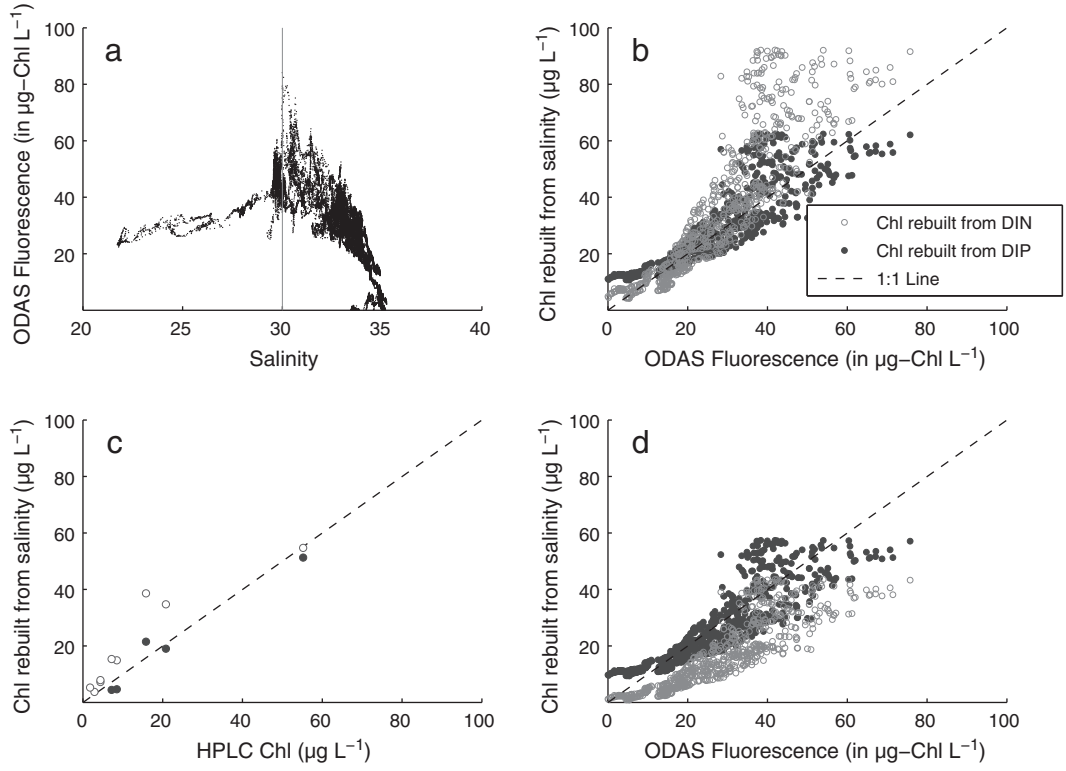

Fig. 12. ODAS-FB data in the BCS (21–25 April 2008). (A) ODAS fluorescence vs. salinity in the continuum of the Belgica cruise trajectory. (B) Comparison of rebuilt *Chlmax* and ODAS fluorescence. *Chlmax* is rebuilt from DIN and from DIP, both of which are rebuilt from spring salinity. The coefficients of the slopes and the offsets derived from in situ data in the year 2008 are used. The correction for the nutrients remaining in the water column is not done as nutrients were not continuously measured together with salinity and fluorescence. The data are aggregated in 1 km-by-1 km squares. (C) Comparison of rebuilt *Chlmax* and in situ chlorophyll *a* (HPLC) in only the few sampling stations where chlorophyll *a* and nutrient concentrations have been measured during the same cruise in April. The correction for the remaining nutrients at the spring biomass peak is done for these stations. (D) Same as (B), except that the multiyear median slopes have been used instead of the 2008 slopes to rebuild *Chlmax* from nutrients (see Table 2, in situ observations in BCS).

Table 3
Nutrients required by phytoplankton to form the spring bloom peak (in the BCS and the DCS) and cellular nutrient ratios of phytoplankton. The spring peak requirements are obtained from the regression slopes of the present study (Figs. 7 and 10), and from the regression slopes derived from results in Muylaert et al. (2006, with permission; data limited to *Phaeocystis* spp. in the Belgian coastal zone). The DIN-to-DIP requirement is the multiyear median of the yearly DIN-to-DIP requirements (see Fig. 10 bottom). The cellular nutrient ratios are obtained from the constants in the MIRO model given in Lancelot et al. (2005), and from the Redfield ratio (assuming a C:Chl ratio of 25 gC $gChl^{-1}$ for growing phytoplankton in the BCS; Lancelot et al., 2005).

Nutrient requirements and nutrient cellular ratios			
	DIN:Chl	DIP:Chl	DIN-to-DIP requirement
Nutrient requirements $(\xi \cdot \kappa)^{-1}$	molN $gChl^{-1}$	molP $gChl^{-1}$	molN $molP^{-1}$
Regression in situ obs. BCS	1.64	2.73E-02	34.4
Regression in situ obs. DCS	0.806	2.50E-02	28.6
Regression Muylaert et al., 2006	2.06	5.99E-02	34.4
Cellular nutrient ratios $(\xi)^{-1}$	molN $gChl^{-1}$	molP $gChl^{-1}$	N-to-P cellular ratio
Model constants in Lancelot et al., 2005	0.51	0.032	15.9
Redfield ratio	0.31	0.020	15.5

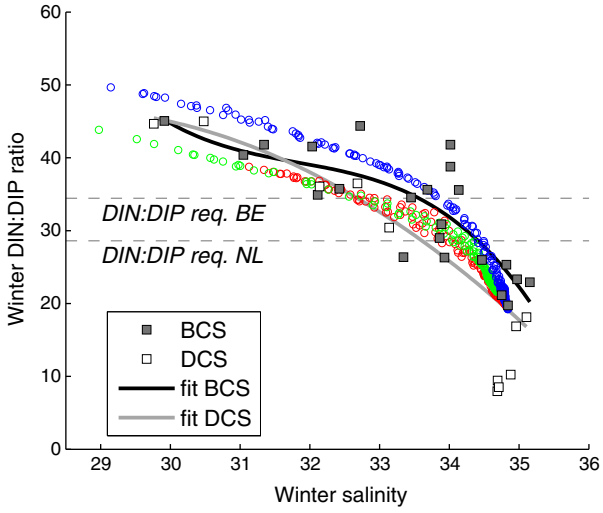

Fig. 13. End-of-winter DIN:DIP ratio (molN $molP^{-1}$) as a function of the end-of-winter salinity for model results (1998 red, 2000 green, 2001 blue), for in situ observations in the BCS (every dot is a multiyear median over 1991–2010 in one of the 23 stations) and for in situ observations in the DCS (multiyear median over 1991–2010 at 12 stations; stations were selected when showing at least 4 values across the period). The fitting curve is a cubic polynomial ($R^2 = 0.67$, rmse = 4.9 molN $molP^{-1}$) for BCS data, and a square polynomial ($R^2 = 0.98$, rmse = 1.8 molN $molP^{-1}$) for DCS data (the latter fitting curve excludes stations Terschelling 100, 135, 175, 235, which are under the influence of North Atlantic and UK river waters with significantly lower winter DIN:DIP ratios; Los et al., 2014). The horizontal lines indicate the DIN-to-DIP requirement for *Chlmax* formation as calculated from in situ data in the BCS and in the DCS (see Table 3).

The long-term average winter DIN:DIP ratio shows a non-linear gradient against salinity that was already observed by De Vries et al. (1998). These authors pointed out that the non-conservative behavior of nutrients illustrates fundamental dynamical properties of estuaries and coastal waters with longer residence times (i.e. adsorption/desorption of phosphate, denitrification, transition from potential P-limitation in spring to potential N-limitation in summer).

4. Discussion

4.1. Predicting chlorophyll a spring maximum from winter DIP

The slope of the '*Chlmax* vs. *Nuteff*' relationship varies from year to year. According to the theory (Eq. (7)), the slope depends on the losses from phytoplankton during the spring bloom formation. The observed interannual variability in the spring-bloom nutrient requirement and, hence, in the losses may be attributed to the variation in the natural assemblage of phytoplankton species. Autolysis, grazing, but also factors such as the carbon-to-chlorophyll ratio will depend on the assemblage of species and their succession in the spring bloom period. In a given year, however, the correlation between *Chlmax* and *Nuteff* is generally high ($R^2 = 0.46$ to 0.98 for DIP in the BCS, see Table 2), in spite of sampling uncertainties. Such a linearity through several sampling stations implies that κ and, hence, the β/α ratio are reasonably constant across the domain in a given year.

Beside exceptional years, DIP requirement shows a lower interannual variability than DIN requirement, which makes winter DIP concentrations and the median DIP requirement a better set of predictors for *Chlmax* in the North Sea continental waters. Now, if the ecosystem were to experience regime shifts affecting its phytoplankton structure the nutrient requirements might be affected as well. Such changes may result, for instance, from reductions in long-term nutrient emissions that would influence the phytoplankton succession/dominance in the coastal zone (see Gypens et al., 2007), or changes that favor nuisance species (Lancelot et al., 2007), or that cause a change in the ecological community structure (Philippart et al., 2007). For instance, if *Phaeocystis* dominance over diatom is enhanced in the future, the DIN-to-DIP requirement might well increase due to *Phaeocystis* affinity for organic phosphorus, as suggested by Fig. 10A (bottom) in 1991.

4.2. Light-limitation, dissolved silica limitation and species succession

It is generally accepted that the onset of the spring phytoplankton bloom is determined by the light availability (Peperzak, 1993; Peperzak et al., 1998). The spring biomass bloom occurs sooner or later in different areas of the North Sea as a function of depth and turbidity. In the present manuscript, the authors focus not on the timing but on the magnitude of the spring maximum of chlorophyll *a*, which is limited by the nutrient availability (Muylaert et al., 2006; Riegman et al., 1992). However, in estuaries and coastal areas the light availability may still be limiting phytoplankton net growth in spring and even in summer when a high turbidity combined with a sufficiently high mixing depth prevents any net phytoplankton production (e.g. De Vries et al., 1998; Desmit et al., 2005; Heip et al., 1995; Loebl et al., 2009; Reid et al., 1990). In these unproductive areas, the observed chlorophyll *a* is exported from adjacent productive areas. In that case, our analysis does not always hold because without any local net production of biomass, the observed chlorophyll *a* and nutrient concentrations may be uncorrelated.

Some previous authors already examined the potential silica (co-)limitation of phytoplankton biomass blooms. The phytoplankton succession in spring from diatoms to *Phaeocystis* is a common pattern in the BCS and DCS and the Si-limitation is linked with the phytoplankton community composition along the seasonal cycle (Baretta-Bekker et al., 2009; Gypens et al., 2007; Loebl et al., 2009; Ly et al., 2014). The present manuscript only focuses on the chlorophyll *a* spring maximum. According to our simple hypothesis, the species succession during the formation of the phytoplankton bloom is not important because the chlorophyll *a* spring maximum is ultimately not Si-limited. As long as DSi remains available, diatom may dominate the spring bloom until exhaustion of another limiting nutrient (DIP or DIN). In contrast, if DSi is depleted before DIP and DIN, a non-diatom species will exhaust DIP or DIN. In any case, the chlorophyll *a* spring maximum will only be interrupted when DIP or DIN is depleted.

Regarding the link between biodiversity and nutrients, recent studies support an inverse direction of causality between phytoplankton diversity and available resource levels (see Ptacnik et al., 2008). "Although diversity was originally considered to depend on available

resource levels […], it is more commonly considered as a driver of ecosystem processes in current biodiversity-ecosystem functioning research" (Olli et al., 2014). This implies that phytoplankton diversity would determine the resource use efficiency and the resulting observable nutrient concentrations. As we did not use any measure of plankton diversity in the present study, we cannot take position in this debate. We simply note that, along the Belgian and Dutch coasts, the nutrients available for the spring bloom are first determined by the riverine inputs. The anthropogenic eutrophication modulated by the hydroclimatic cycles recurrently results in a dramatic spring dominance of the opportunistic species *Phaeocystis* (Baretta-Bekker et al., 2009; Breton et al., 2006; Lancelot et al., 1987; Riegman et al., 1992).

4.3. Predicted nutrient limitation of Chlmax

To enhance the quality of the *Chlmax* prediction, the estimate should better be made on the sole basis of the limiting nutrient. Over the period 1990–2005, Loebl et al. (2009) identified DIP as a potential limiting (or co-limiting) factor in most coastal areas of the North Sea from Belgium to Denmark. In the BCS (station 330), the authors consistently identified DIP and DSi as potential limiting nutrients in spring and summer over the period. Exceptionally, they also observe a potential nitrogen limitation at station 330 at the end of the spring 1998. In the present study, the model runs made in the years 2000 and 2001 show that DIP is consistently limiting the chlorophyll *a* spring bloom at station 330. However, in 1998, the modeled salinity isoline (not shown) at which the switch in nutrient limitation is predicted (Fig. 13) was singularly close to the coast due to a pulse of oceanic inflow into the North Sea. That year, an increase in the flow of the European shelf-edge current was observed (Beaugrand, 2004; Holliday and Reid, 2001). Therefore, our results predicted a N-limitation at station 330 in 1998, which supports conclusions of Loebl et al. (2009) and confirms that the nutrient limitation of phytoplankton production is salinity-dependent in this area.

In Muylaert et al. (2006), the spring *Phaeocystis* bloom of 2003 has been observed in situ in the Belgian coastal zone. By comparing the March nutrient concentrations to *Phaeocystis* half-saturation constants for nutrient uptake, the authors observe in some stations that the DIP in March is smaller than the half-saturation constant for P-uptake, whereas it is not the case for DIN. They conclude that "the magnitude of the *Phaeocystis* spring bloom in 2003 was regulated by phosphorus rather than nitrogen" in the coastal zone. This conclusion based on the knowledge of the half-saturation constant goes in the same direction as the results of the present study, which is solely based on nutrient requirements.

With a combination of several techniques, Ly et al. (2014) carefully investigated which factor was limiting phytoplankton biomass in April 2010 at a coastal station close to Marsdiep (western Wadden Sea). They concluded that the natural assemblage of phytoplankton in April was mainly P-limited (with a co-limitation of P and Si for diatoms), which corroborates our results. They also pointed out that P-limited phytoplankton is able to mobilize phosphorus from dissolved organic phosphorus (DOP) compounds through the alkaline phosphatase activity (APA), and that algal species may differ in their APA regulatory response. That observation does not weaken our prediction of DIP requirement from winter DIP because APA would only start to be a significant alternative source of P when DIP is depleted, i.e. just after the spring bloom peak. Also, Ly et al. (2014) concluded that the DIN:DIP ratio remains the best predictor of the nature of the limiting nutrient in a spring phytoplankton bloom, which further supports our study.

Previous model studies with the 0-D biological model MIRO (Lancelot et al., 2005) also analyzed the limiting factors for phytoplankton production. Gypens et al. (2007) estimated that a change in nutrient limitation occurred during the 1990's. Before 1993, spring diatoms were limited by DSi and *Phaeocystis* colonies by DIN. After 1993, both the spring diatoms and the *Phaeocystis* colonies turned out to be limited by DIP. The change resulted from a progressive DIN:DIP increase in the BCS waters following the phosphate reduction policies in most European continental rivers (Vermaat et al., 2008). The present study also concludes at a consistent P-limitation in the coastal continental waters of the North Sea in recent years.

With a slightly different version of the model 3D-MIRO&CO (see Section 2.5), Lacroix et al. (2007a) identified a limitation of *Phaeocystis* colonies by DIN in both the coastal and offshore areas of the BCS. These results are in contrast to the ones of the present study. When considering that *Phaeocystis* colonies dominate the chlorophyll *a* spring maximum, then *Phaeocystis* colonies in the present study are expected to be P-limited in the coastal zone at salinities lower than 34 psu (Fig. 13). The slight changes in the model versions do not explain such a disagreement in the conclusions about nutrient limitations. The difference may come from the methods used to estimate the nutrient limitations. Lacroix et al. (2007a) reproduced a limitation function that is used by the model itself (see Lancelot et al., 2005). The limitation function is based on the instantaneous nutrient concentrations and on the half-saturation constants for nutrient uptake by phytoplankton. Time series of the limitation functions per species were used to identify the limiting nutrient at the biomass bloom peak. However, in 3D-MIRO&CO, the net phytoplankton growth is not regulated directly by the limitation function but rather by a complex combination of growth and loss rates, which are themselves modulated by the limitation function. A careful examination at the modeled time series of the limitation function together with the time series of growth and loss rates (not shown) allowed identifying a P-limitation for *Phaeocystis* at station 330 (coastal zone), and a N-limitation in the offshore close to the boundary of the BCS. It is concluded that the method proposed in this study to predict the limiting nutrient for *Chlmax* on the basis of the nutrient requirements is in accordance with the examination of the modeled growth and loss fluxes, and not in accordance with the limitation function used in Lacroix et al. (2007a).

4.4. Priority in nutrient reductions

Since the early 1990's, the chlorophyll *a* spring maximum has likely been limited by phosphorus in the southern North Sea continental coasts. Historical changes in nutrient emissions have an impact on the nutrient limitation in the North Sea (Gypens et al., 2007; Lancelot et al., 2007). Supporting the idea that alleviation of eutrophication often requires a dual-nutrient-reduction strategy (see Conley et al., 2009), the present study calls for controlled reduction of phosphorus and nitrogen emissions to the sea. Phosphorus could be reduced as it controls the size of the phytoplankton spring bloom in the coastal zone. At the same time, nitrogen must be reduced in order to limit the capacity of *Phaeocystis* to grow under low phosphorus concentrations and dominate the spring bloom (see also Gypens et al., 2007; Lacroix et al., 2007a). It should be pointed out that further P reduction without concomitant N reduction may negatively affect diatoms before canceling *Phaeocystis* nuisance (Gypens et al., 2007). The analysis of long-time series records in the DCS further supports N reduction for the lone purpose of limiting *Phaeocystis* growth (Prins et al., 2012). An increase in dissolved silica has been recorded since 1990 in the DCS, and it coincided with increased diatom biomass and increased occurrence of dense diatom blooms. However, the concomitant decrease in N:Si ratio did not result apparently in a reduction of *Phaeocystis* growth through competition for resources. This suggests that a reduction in nitrogen riverine loads is still necessary to limit *Phaeocystis* growth in the Dutch coastal zone. A clue on the relative nutrient target levels to be reached is suggested in Fig. 13. While keeping phosphorus low, if the winter DIN:DIP in the coastal zone were to decrease towards or below 34.4 molN $molP^{-1}$ in the BCS, or 28.6 molN $molP^{-1}$ in the DCS, the system would probably favor phytoplankton assemblages similar to

the ones found in the Belgian and Dutch offshore zones, where colonial *Phaeocystis* is not a nuisance (Gypens et al., 2007; Lancelot et al., 2009).

4.5. Application to other marine systems

The method developed in this study does not require complex models and may be applied on existing historical datasets containing winter and spring values for salinity, nutrient and chlorophyll *a* concentrations. It may potentially be extended to other marine systems, provided their winter and spring nutrient concentrations are mainly determined by two end-members, for instance river-ocean systems. In this study, the method has been applied in vertically well-mixed systems and the authors do not know how the method would apply in stratified systems.

Acknowledgments

This work has been carried out in the framework of the AMORE III project, funded by the Belgian Science Policy Office (BELSPO : SD/NS/03A), and by the FP7 CoBiOS project (EU-FP7-SPACE-2010-1, project CoBiOS : Project number 263295), and by the EMoSEM project (EU-FP7-ERANET Seas-era project funded by BELSPO, SD/ER/11). The in situ observations in the BCS were measured by the RBINS/MARCHEM team and by the laboratory Ecology of Aquatic Systems, Université Libre de Bruxelles. They are available at the Belgian Marine Data Center (BMDC; www.bmdc.be). The authors are grateful to the RV Belgica and the Meetdienst Oostende for providing ODAS-FB data. In situ observation data in the DCS are available on http://live.waterbase.nl, and the authors are grateful to Hans Los and Theo Prins (Deltares) for providing consistent datasets. The authors would also like to thank the SOMLIT, the "Service d'Observation en Milieu Littoral", INSU-CNRS, Roscoff, for the provision of data in the French coastal zone and English Channel. The authors are grateful to the two anonymous reviewers for their useful comments.

References

Baretta-Bekker, J.G., Baretta, J.W., Latuhihin, M.J., Desmit, X., Prins, T.C., 2009. Description of the long-term (1991–2005) temporal and spatial distribution of phytoplankton carbon biomass in the Dutch North Sea. J. Sea Res. 61, 50–59.

Beaugrand, G., 2004. The North Sea regime shift: evidence, causes, mechanisms and consequences. Prog. Oceanogr. 60, 245–262.

Breton, E., Rousseau, V., Parent, J.-Y., Ozer, J., Lancelot, C., 2006. Hydroclimatic modulation of the diatom/*Phaeocystis* blooms in the nutrient-enriched Belgian coastal waters (North Sea). Limnol. Oceanogr. 51, 1–14.

Brion, N., Jans, S., Chou, L., Rousseau, V., 2006. Nutrient loads to the Belgian coastal zone. In: Rousseau, V., Lancelot, C., Cox, D. (Eds.), Current Status of Eutrophication in the Belgian Coastal Zone. Presses Universitaires de Bruxelles, Bruxelles, pp. 17–43.

Brussaard, C.P.D., Riegman, R., Noordeloos, A.A.M., Cadée, G.C., Witte, H., Kop, A.J., Nieuwland, G., van Duyl, F.C., Bak, R.P.M., 1995. Effects of grazing, sedimentation and phytoplankton cell lysis on the structure of a coastal pelagic food web. Mar. Ecol. Prog. Ser. 123, 259–271.

Cadée, G.C., Hegeman, J., 2002. Phytoplankton in the Marsdiep at the end of the 20th century; 30 years monitoring biomass, primary production, and *Phaeocystis* blooms. J. Sea Res. 48, 97–110.

Conley, D.J., Paerl, H.W., Howarth, R.W., Boesch, D.F., Seitzinger, S.P., Havens, K.E., Lancelot, C., Likens, G.E., 2009. Controlling eutrophication: nitrogen and phosphorus. Science 323 (5917), 1014–1015.

Daro, M.-H., Breton, E., Antajan, E., Gasparini, S., Rousseau, V., 2006. Do *Phaeocystis* colony blooms affect zooplankton in the Belgian coastal zone? In: Rousseau, V., Lancelot, C., Cox, D. (Eds.), Current Status of Eutrophication in the Belgian Coastal Zone. Presses Universitaires de Bruxelles, Bruxelles, pp. 61–72

de Vries, I., Duin, R.N.M., Peeters, J.C.H., Los, F.J., Bokhorst, M., Laane, R.W.P.M., 1998. Patterns and trends in nutrients and phytoplankton in Dutch coastal waters: comparison of time-series analysis, ecological model simulation, and mesocosm experiments. ICES J. Mar. Sci. 55, 620–634.

Desmit, X., Vanderborght, J.P., Regnier, P., Wollast, R., 2005. Control of phytoplankton production by physical forcing in a strongly tidal, well-mixed estuary. Biogeosciences 2, 205–218.

Gieskes, W.W.C., Schaub, B.E.M., 1990. Correlation of the Seasonal and Annual Variation of Phytoplankton Biomass in Dutch Coastal Waters of the North Sea with Rhine River Discharge. Springer-Verlag, Berlin, pp. 311–320.

Gypens, N., Lacroix, G., Lancelot, C., 2007. Causes of variability in diatom and *Phaeocystis* blooms in Belgian coastal waters between 1989 and 2003: a model study. J. Sea Res. 57, 19–35.

Heip, C.H.R., Goosen, N., Herman, P.M.J., Kromkamp, J., Middelburg, J.J., Soetaert, K., 1995. Production and consumption of biological particles in temperate tidal estuaries. Oceanogr. Mar. Biol. Annu. Rev. 33, 1–149.

Henriksen, P., 2009. Long-term changes in phytoplankton in the Kattegat, the Belt Sea, the Sound and the western Baltic Sea. J. Sea Res. 61, 114–123.

Holliday, N.P., Reid, P.C., 2001. Is there a connection between high transport of water through the Rockall Trough and ecological changes in the North Sea? ICES J. Mar. Sci. 58, 270–274.

Jickells, T.D., 1998. Nutrient biogeochemistry of the coastal zone. Science 281, 217.

Lacroix, G., Ruddick, K., Ozer, J., Lancelot, C., 2004. Modelling the impact of the Scheldt and Rhine/Meuse plumes on the salinity distribution in Belgian waters (southern North Sea). J. Sea Res. 52, 149–163.

Lacroix, G., Ruddick, K., Gypens, N., Lancelot, C., 2007a. Modelling the relative impact of rivers (Scheldt/Rhine/Seine) and Channel water on the nutrient and diatoms/*Phaeocystis* distributions in Belgian waters (Southern North Sea). Cont. Shelf Res. 27, 1422–1446.

Lacroix, G., Ruddick, K., Park, Y., Gypens, N., Lancelot, C., 2007b. Validation of the 3D biogeochemical model MIRO&CO with field nutrient and phytoplankton data and MERIS-derived surface chlorophyll *a* images. J. Mar. Syst. 64, 66–88.

Lancelot, C., Billen, G., Sournia, A., Weisse, T., Colijn, F., Veldhuis, M.J.W., Davies, A., Wassman, P., 1987. *Phaeocystis* blooms and nutrient enrichment in the continental coastal zones of the North Sea. Ambio 16, 38–46.

Lancelot, C., Spitz, Y., Gypens, N., Ruddick, K., Becquevort, S., Rousseau, V., Lacroix, G., Billen, G., 2005. Modelling diatom and *Phaeocystis* blooms and nutrient cycles in the Southern Bight of the North Sea: the MIRO model. Mar. Ecol. Prog. Ser. 289, 63–78.

Lancelot, C., Gypens, N., Billen, G., Garnier, J., Roubeix, V., 2007. Testing an integrated river-ocean mathematical tool for linking marine eutrophication to land use: the *Phaeocystis*-dominated Belgian coastal zone (Southern North Sea) over the past 50 years. J. Mar. Syst. 64, 216–228.

Lancelot, C., Rousseau, V., Gypens, N., 2009. Ecologicaly based indicators for *Phaeocystis* disturbance in eutrophied Belgian coastal waters (Southern North Sea) based on field observations and ecological modelling. J. Sea Res. 61, 44–49.

Loebl, M., Colijn, F., Van Beusekom, J.E.E., Barreta-Bekker, J.G., Lancelot, C., Philippart, C.J.M., Rousseau, V., Wiltshire, K.H., 2009. Recent patterns in potential phytoplankton limitation along the Northwest European continental coast. J. Sea Res. 61, 34–43.

Los, F.J., Bokhorst, M., 1997. Trend analysis Dutch coastal zone. New Challenges for North Sea Research. Zentrum for Meeres- und Klimaforschung, University of Hamburg, pp. 161–175.

Los, F.J., Troost, T.A., Van Beek, J.K.L., 2014. Finding the optimal reduction to meet all targets — applying linear programming with a nutrient tracer model of the North Sea. J. Mar. Syst. 131, 91–101.

Luyten, P.J., Jones, J.E., Proctor, R., Tabor, A., Tett, P., Wild-Allen, K., 1999. COHERENS Documentation: a Coupled Hydrodynamical-ecological Model for Regional and Shelf Seas: User Documentation. MUMM, Brussels, p. 903.

Ly, J., Philippart, C.J.M., Kromkamp, J.C., 2014. Phosphorus limitation during a phytoplankton spring bloom in the western Dutch Wadden Sea. J. Sea Res. 88, 109–120.

Mieruch, S., Freund, J.A., Feudel, U., Boersma, M., Janisch, S., Wiltshire, K.H., 2010. A new method of describing phytoplankton blooms: examples from Helgoland Roads. J. Mar. Syst. 79, 36–43.

Muylaert, K., Gonzales, R., Franck, M., Lionard, M., Van der Zee, C., Cattrijsse, A., Sabbe, K., Chou, L., Vyverman, W., 2006. Spatial variation in phytoplankton dynamics in the Belgian coastal zone of the North Sea studied by microscopy, HPLC-CHEMTAX and underway fluorescence recordings. J. Sea Res. 55, 253–265.

Olli, K., Ptacnik, R., Andersen, T., Trikk, O., Klais, R., Lehtinen, S., Tamminen, T., 2014. Against the tide: recent diversity increase enhances resource use in a coastal ecosystem. Limnol. Oceanogr. 59 (1), 267–274.

Peperzak, L., 1993. Daily irradiance governs growth rate and colony formation of *Phaeocystis* (Prymnesiophycae). J. Plankton Res. 15, 809–821.

Peperzak, L., Colijn, F., Gieskes, W.W.C., Peeters, J.C.H., 1998. Development of the diatom-*Phaeocystis* spring bloom in the Dutch coastal zone of the North Sea: the silicon depletion versus the daily irradiance threshold hypothesis. J. Plankton Res. 20, 517–537.

Philippart, C.J.M., Beukema, J.J., Cadée, G.C., Dekker, R., Goedhart, P.W., van Iperen, J.M., Leopold, M.F., Herman, P.M.J., 2007. Impacts of nutrient reduction on coastal communities. Ecosystems 10, 95–118.

Prins, T.C., Desmit, X., Baretta-Bekker, J.G., 2012. Phytoplankton composition in Dutch coastal waters responds to changes in riverine nutrient loads. J. Sea Res. 73, 49–62.

Ptacnik, R., Solimini, A.G., Andersen, T., Tamminen, T., Brettum, P., Lepistö, L., Willén, E., Rekolainen, S., 2008. Diversity predicts stability and resource use efficiency in natural phytoplankton communities. Proc. Natl. Acad. Sci. U. S. A. 105, 5134–5138. http://dx.doi.org/10.1073/pnas.0708328105.

Reid, P.C., Lancelot, C., Gieskes, W.W.C., Hagmeier, E., Weichart, G., 1990. Phytoplankton of the North Sea and its dynamics: a review. J. Sea Res. 26, 295–331.

Riegman, R., Noordeloos, A.A.M., Cadée, G.C., 1992. *Phaeocystis* blooms and eutrophication of the continental coastal zones of the North Sea. Mar. Biol. 112, 479–484.

Rousseau, V., Becquevort, S., Parent, J.-Y., Gasparini, S., Daro, M.-H., Tackx, M., Lancelot, C., 2000. Trophic efficiency of the planktonic food web in a coastal ecosystem dominated by *Phaeocystis* colonies. J. Sea Res. 43, 357–372.

Rousseau, V., Park, Y., Ruddick, K., Vyverman, W., Parent, J.-Y., Lancelot, C., 2006. Phytoplankton blooms in response to nutrient enrichment. In: Rousseau, V., Lancelot, C., Cox, D. (Eds.), Current Status of Eutrophication in the Belgian Coastal Zone. Presses Universitaires de Bruxelles, Bruxelles, pp. 45–59.

Rousseau, V., Lantoine, F., Rodriguez, F., LeGall, F., Chrétiennot-Dinet, M.-J., Lancelot, C., 2012. Characterization of *Phaeocystis globosa* (Prymnesiophyceae), the blooming species in the Southern North Sea. J. Sea Res. 76, 105–113.

Ruddick, K., Lacroix, G., 2006. Hydrodynamics and meteorology of the Belgian Coastal Zone. In: Rousseau, V., Lancelot, C., Cox, D. (Eds.), Current Status of Eutrophication in the Belgian Coastal Zone. Presses Universitaires de Bruxelles, Bruxelles, pp. 1–15.

Schaub, B.E.M., Gieskes, W.W.C., 1991. Eutrophication of the North Sea: the relation between Rhine river discharge and chlorophyll-a concentration in Dutch coastal waters. In: Elliott en, M., Ducrotoy, J.-P. (Eds.), Estuaries and Coasts: Spatial and Temporal Intercomparisons. Olsen & Olsen, Fredensborg, pp. 85–90.

Schoemann, V., Becquevort, S., Stefels, J., Rousseau, V., Lancelot, C., 2005. *Phaeocystis* blooms in the global ocean and their controlling mechanisms: a review. J. Sea Res. 53, 43–66.

Sirjacobs, D., Alvera-Azcárate, A., Barth, A., Lacroix, G., Park, Y., Nechad, B., Ruddick, K., Beckers, J.-M., 2011. Cloud filling of ocean colour and sea surface temperature remote sensing products over the Southern North Sea by the data interpolating empirical orthogonal functions methodology. J. Sea Res. 65, 114–130.

Soetaert, K., Middelburg, J.J., Heip, C., Meire, P., Van Damme, S., Maris, T., 2006. Long-term change in dissolved inorganic nutrients in the heterotrophic Scheldt estuary (Belgium, The Netherlands). Limnol. Oceanogr. 51, 409–423.

Thieu, V., Garnier, J., Billen, G., 2010. Assessing the effect of nutrient mitigation measures in the watersheds of the Southern Bight of the North Sea. Sci. Total Environ. 408, 1245–1255.

van Beusekom, J.E.E., Loebl, M., Martens, P., 2009. Distant riverine nutrient supply and local temperature drive the long-term phytoplankton development in a temperate coastal basin. J. Sea Res. 61, 26–33.

Vermaat, J.E., McQuatters-Gollop, A., Eleveld, M.A., Gilbert, A.J., 2008. Past, present and future nutrient loads of the North Sea: causes and consequences. Estuar. Coast. Shelf Sci. 80 (1), 53–59.

Wollast, R., 2003. Biogeochemical processes in estuaries. Marine science frontiers for Europe. In: Wefer, G., Lamy, F., Mantoura, F. (Eds.), Springer-Verlag Berlin Heidelberg, New York Tokyo, pp. 61–77.